verse the impaired bone growth observed in Ach mice [50]. The safety of systemic CNP administration in preclinical studies with the observation that CNP has only a minimal effect of blood pressure in humans [51] suggests that systemic administration of CNP provides a novel therapeutic strategy for the treatment of human skeletal dysplasias including achondroplasia.

III. Future direction of CNP therapy for skeletal dysplasias

Currently, the primary target of the translational research of CNP is achondroplasia. The efficacy of CNP therapy for achondroplasia has been demonstrated by preclinical studies using its mice model. As CNP has a strong stimulatory effect on the growth of bones of wild-type mice [49], it is expected that CNP therapy is effective for the treatment of skeletal dysplasias other than achondroplasia. Nevertheless, it is supposed that CNP therapy is not effective for acromesomelic dysplasia type Maroteaux, which is caused by loss-of-function mutations in the GC-B gene. In order to select forms of skeletal dysplasias which will be applied for CNP therapy, we must further establish the proof-of-concept of CNP therapy for skeletal dysplasias other than achondroplasia.

Because CNP is an intrinsic peptide, the possibility of the safety of CNP therapy might be considerably high. On the other hand, as is in common for peptide drugs, CNP may easily be degraded by endopeptidases. Accordingly, we will have to try to explore various strategies to activate the CNP/GC-B system: for example, inhibition of endopeptidases or blockade of C-receptor, specifically in the growth plate, might be included.

In conclusion, we have discovered that the CNP/GC-B system is a potent stimulator of endochondral bone growth by using transgenic and knockout mice. The translational research of this effect into skeletal dysplasias, including achondroplasia, is now ongoing in our laboratory.

References

1. Nakao K, Ogawa Y, Suga S, Imura H (1992) Molecular biology and biochemistry of the natriuretic peptide system. I: Natriuretic peptides. *J Hypertens* 10:907-912.
2. Nakao K, Ogawa Y, Suga S, Imura H (1992) Molecular biology and biochemistry of the natriuretic peptide system. II: Natriuretic peptide receptors. *J Hypertens* 10:1111-1114.
3. Suga S, Nakao K, Hosoda K, Mukoyama M, Ogawa Y, Shirakami G, Arai H, Saito Y, Kambayashi Y, Inouye K, et al. (1992) Receptor selectivity of natriuretic peptide family, atrial natriuretic peptide, brain natriuretic peptide, and C-type natriuretic peptide. *Endocrinology* 130:229-239.
4. Sugawara A, Nakao K, Morii N, Yamada T, Itoh H, Shiono S, Saito Y, Mukoyama M, Arai H, Nishimura K, *et al.* (1988) Synthesis of atrial natriuretic polypeptide in human failing hearts. Evidence for altered processing of atrial natriuretic polypeptide precursor and augmented synthesis of beta-human ANP. *J Clin Invest* 81:1962-1970.
5. Saito Y, Nakao K, Arai H, Nishimura K, Okumura K, Obata K, Takemura G, Fujiwara H, Sugawara A, Yamada T, *et al.* (1989) Augmented expression of atrial natriuretic polypeptide gene in ventricle of human failing heart. *J Clin Invest* 83:298-305.
6. Mukoyama M, Nakao K, Saito Y, Ogawa Y, Hosoda K, Suga S, Shirakami G, Jougasaki M, Imura H (1990) Human brain natriuretic peptide, a novel cardiac hormone. *Lancet* 335:801-802.
7. Mukoyama M, Nakao K, Saito Y, Ogawa Y, Hosoda K, Suga S, Shirakami G, Jougasaki M, Imura H (1990) Increased human brain natriuretic peptide in congestive heart failure. *N Engl J Med* 323:757-758.
8. Mukoyama M, Nakao K, Hosoda K, Suga S, Saito Y, Ogawa Y, Shirakami G, Jougasaki M, Obata K, Yasue H, *et al.* (1991) Brain natriuretic peptide as a novel cardiac hormone in humans. Evidence for an exquisite dual natriuretic peptide system, atrial natriuretic peptide and brain natriuretic peptide. *J Clin Invest* 87:1402-1412.
9. Morita E, Yasue H, Yoshimura M, Ogawa H, Jougasaki M, Matsumura T, Mukoyama M, Nakao K (1993) Increased plasma levels of brain natriuretic peptide in patients with acute myocardial infarction. *Circulation* 88:82-91.
10. Kawakami R, Saito Y, Kishimoto I, Harada M, Kuwahara K, Takahashi N, Nakagawa Y, Nakanishi M, Tanimoto K, Usami S, Yasuno S, Kinoshita H, Chusho H, Tamura N, Ogawa Y, Nakao K (2004) Overexpression of brain natriuretic peptide facilitates neutrophil infiltration and cardiac matrix metalloproteinase-9 expression after acute myocardial infarction.

Circulation 110:3306-3312.

11. Arai H, Nakao K, Saito Y, Morii N, Sugawara A, Yamada T, Itoh H, Shiono S, Mukoyama M, Ohkubo H, *et al.* (1988) Augmented expression of atrial natriuretic polypeptide gene in ventricles of spontaneously hypertensive rats (SHR) and SHR-stroke prone. *Circ Res* 62:926-930.
12. Yasue H, Yoshimura M, Sumida H, Kikuta K, Kugiyama K, Jougasaki M, Ogawa H, Okumura K, Mukoyama M, Nakao K (1994) Localization and mechanism of secretion of B-type natriuretic peptide in comparison with those of A-type natriuretic peptide in normal subjects and patients with heart failure. *Circulation* 90:195-203.
13. Sugawara A, Nakao K, Sakamoto M, Morii N, Yamada T, Itoh H, Shiono S, Imura H (1985) Plasma concentration of atrial natriuretic polypeptide in essential hypertension. *Lancet* Dec 21-28;2:1426-1427.
14. Itoh H, Nakao K, Mukoyama M, Yamada T, Hosoda K, Shirakami G, Morii N, Sugawara A, Saito Y, Shiono S, *et al.* (1989) Chronic blockade of endogenous atrial natriuretic polypeptide (ANP) by monoclonal antibody against ANP accelerates the development of hypertension in spontaneously hypertensive and deoxycorticosterone acetate-salt-hypertensive rats. *J Clin Invest* 84:145-154.
15. Ogawa Y, Nakao K, Mukoyama M, Hosoda K, Shirakami G, Arai H, Saito Y, Suga S, Jougasaki M, Imura H (1991) Natriuretic peptides as cardiac hormones in normotensive and spontaneously hypertensive rats. The ventricle is a major site of synthesis and secretion of brain natriuretic peptide. *Circ Res* 69:491-500.
16. Saito Y, Nakao K, Nishimura K, Sugawara A, Okumura K, Obata K, Sonoda R, Ban T, Yasue H, Imura H (1987) Clinical application of atrial natriuretic polypeptide in patients with congestive heart failure: beneficial effects on left ventricular function. *Circulation* 76:115-124.
17. Yoshimura M, Yasue H, Morita E, Sakaino N, Jougasaki M, Kurose M, Mukoyama M, Saito Y, Nakao K, Imura H (1991) Hemodynamic, renal, and hormonal responses to brain natriuretic peptide infusion in patients with congestive heart failure. *Circulation* 84:1581-1588.
18. Sudoh T, Minamino N, Kangawa K, Matsuo H (1990) C-type natriuretic peptide (CNP): a new member of natriuretic peptide family identified in porcine brain. *Biochem Biophys Res Commun* 168:863-870.
19. Komatsu Y, Nakao K, Suga S, Ogawa Y, Mukoyama M, Arai H, Shirakami G, Hosoda K, Nakagawa O, Hama N, et al. (1991) C-type natriuretic peptide (CNP) in rats and humans. *Endocrinology* 129:1104-1106.
20. Suga S, Nakao K, Itoh H, Komatsu Y, Ogawa Y, Hama N, Imura H (1992) Endothelial production of C-type natriuretic peptide and its marked augmentation by transforming growth factor-beta. Possible existence of "vascular natriuretic peptide system". *J Clin Invest* 90:1145-1149.
21. Suga S, Itoh H, Komatsu Y, Ogawa Y, Hama N, Yoshimasa T, Nakao K (1993) Cytokine-induced C-type natriuretic peptide (CNP) secretion from vascular endothelial cells--evidence for CNP as a novel autocrine/paracrine regulator from endothelial cells. *Endocrinology* 133:3038-3041.
22. Doi K, Itoh H, Komatsu Y, Igaki T, Chun T H, Takaya K, Yamashita J, Inoue M, Yoshimasa T, Nakao K (1996) Vascular endothelial growth factor suppresses C-type natriuretic peptide secretion. *Hypertension* 27:811-815.
23. Kubo A, Isumi Y, Ishizaka Y, Tomoda Y, Kangawa K, Dohi K, Matsuo H, Minamino N (2001) C-type natriuretic peptide is synthesized and secreted from leukemia cell lines, peripheral blood cells, and peritoneal macrophages. *Exp Hematol* 29:609-615.
24. Chusho H, Tamura N, Ogawa Y, Yasoda A, Suda M, Miyazawa T, Nakamura K, Nakao K, Kurihara T, Komatsu Y, Itoh H, Tanaka K, Saito Y, Katsuki M, Nakao K (2001) Dwarfism and early death in mice lacking C-type natriuretic peptide. *Proc Natl Acad Sci U S A* 98:4016-4021.
25. Kronenberg H M (2003) Developmental regulation of the growth plate. *Nature* 423:332-336.
26. Tamura N, Doolittle L K, Hammer R E, Shelton J M, Richardson J A, Garbers D L (2004) Critical roles of the guanylyl cyclase B receptor in endochondral ossification and development of female reproductive organs. *Proc Natl Acad Sci U S A* 101:17300-17305.
27. Yasoda A, Komatsu Y, Chusho H, Miyazawa T, Ozasa A, Miura M, Kurihara T, Rogi T, Tanaka S, Suda M, Tamura N, Ogawa Y, Nakao K (2004) Overexpression of CNP in chondrocytes rescues achondroplasia through a MAPK-dependent pathway. *Nat Med* 10:80-86.
28. Feil R, Lohmann S M, de Jonge H, Walter U, Hofmann F (2003) Cyclic GMP-dependent protein kinases and the cardiovascular system: insights from genetically modified mice. *Circ Res* 93:907-916.
29. Pfeifer A, Aszodi A, Seidler U, Ruth P, Hofmann F, Fassler R (1996) Intestinal secretory defects and dwarfism in mice lacking cGMP-dependent protein kinase II. *Science* 274:2082-2086.
30. Miyazawa T, Ogawa Y, Chusho H, Yasoda A, Tamura N, Komatsu Y, Pfeifer A, Hofmann F, Nakao K (2002) Cyclic GMP-dependent protein kinase II plays a critical role in C-type natriuretic peptide-mediated endochondral ossification. *Endocrinology* 143:3604-3610.
31. Kawasaki Y, Kugimiya F, Chikuda H, Kamekura S, Ikeda T, Kawamura N, Saito T, Shinoda Y, Higashikawa A, Yano F, Ogasawara T, Ogata N, Hoshi K, Hofmann F, Woodgett J R, Nakamura K, Chung U I, Kawaguchi H (2008) Phosphorylation of GSK-3beta by cGMP-dependent protein kinase II promotes hypertrophic differentiation of murine chondrocytes. *J Clin*

Invest 118:2506-2515.
32. Matsukawa N, Grzesik W J, Takahashi N, Pandey K N, Pang S, Yamauchi M, Smithies O (1999) The natriuretic peptide clearance receptor locally modulates the physiological effects of the natriuretic peptide system. *Proc Natl Acad Sci U S A* 96:7403-7408.
33. Moffatt P, Thomas G, Sellin K, Bessette M C, Lafreniere F, Akhouayri O, St-Arnaud R, Lanctot C (2007) Osteocrin is a specific ligand of the natriuretic Peptide clearance receptor that modulates bone growth. *J Biol Chem* 282:36454-36462.
34. Tsuji T, Kunieda T (2005) A loss-of-function mutation in natriuretic peptide receptor 2 (Npr2) gene is responsible for disproportionate dwarfism in cn/cn mouse. *J Biol Chem* 280:14288-14292.
35. Sogawa C, Tsuji T, Shinkai Y, Katayama K, Kunieda T (2007) Short-limbed dwarfism: slw is a new allele of Npr2 causing chondrodysplasia. *J Hered* 98:575-580.
36. Tsuji T, Kondo E, Yasoda A, Inamoto M, Kiyosu C, Nakao K, Kunieda T (2008) Hypomorphic mutation in mouse Nppc gene causes retarded bone growth due to impaired endochondral ossification. *Biochem Biophys Res Commun* 376:186-190.
37. Jiao Y, Yan J, Jiao F, Yang H, Donahue L R, Li X, Roe B A, Stuart J, Gu W (2007) A single nucleotide mutation in Nppc is associated with a long bone abnormality in lbab mice. *BMC Genet* 8:16.
38. Chikuda H, Kugimiya F, Hoshi K, Ikeda T, Ogasawara T, Shimoaka T, Kawano H, Kamekura S, Tsuchida A, Yokoi N, Nakamura K, Komeda K, Chung U I, Kawaguchi H (2004) Cyclic GMP-dependent protein kinase II is a molecular switch from proliferation to hypertrophic differentiation of chondrocytes. *Genes Dev* 18:2418-2429.
39. Jaubert J, Jaubert F, Martin N, Washburn L L, Lee B K, Eicher E M, Guenet J L (1999) Three new allelic mouse mutations that cause skeletal overgrowth involve the natriuretic peptide receptor C gene (Npr3). *Proc Natl Acad Sci U S A* 96:10278-10283.
40. Bartels C F, Bukulmez H, Padayatti P, Rhee D K, van Ravenswaaij-Arts C, Pauli R M, Mundlos S, Chitayat D, Shih L Y, Al-Gazali L I, Kant S, Cole T, Morton J, Cormier-Daire V, Faivre L, Lees M, Kirk J, Mortier G R, Leroy J, Zabel B, Kim C A, Crow Y, Braverman N E, van den Akker F, Warman M L (2004) Mutations in the transmembrane natriuretic peptide receptor NPR-B impair skeletal growth and cause acromesomelic dysplasia, type Maroteaux. *Am J Hum Genet* 75:27-34.
41. Olney R C, Bukulmez H, Bartels C F, Prickett T C, Espiner E A, Potter L R, Warman M L (2006) Heterozygous mutations in natriuretic peptide receptor-B (NPR2) are associated with short stature. *J Clin Endocrinol Metab* 91:1229-1232.
42. Bocciardi R, Giorda R, Buttgereit J, Gimelli S, Divizia M T, Beri S, Garofalo S, Tavella S, Lerone M, Zuffardi O, Bader M, Ravazzolo R, Gimelli G (2007) Overexpression of the C-type natriuretic peptide (CNP) is associated with overgrowth and bone anomalies in an individual with balanced t(2;7) translocation. *Hum Mutat* 28:724-731.
43. Moncla A, Missirian C, Cacciagli P, Balzamo E, Legeai-Mallet L, Jouve J L, Chabrol B, Le Merrer M, Plessis G, Villard L, Philip N (2007) A cluster of translocation breakpoints in 2q37 is associated with overexpression of NPPC in patients with a similar overgrowth phenotype. *Hum Mutat* 28:1183-1188.
44. Superti-Furga A, Bonafe L, Rimoin D L (2001) Molecular-pathogenetic classification of genetic disorders of the skeleton. *Am J Med Genet* 106:282-293.
45. Rousseau F, Bonaventure J, Legeai-Mallet L, Pelet A, Rozet J M, Maroteaux P, Le Merrer M, Munnich A (1994) Mutations in the gene encoding fibroblast growth factor receptor-3 in achondroplasia. *Nature* 371:252-254.
46. Cattaneo R, Villa A, Catagni M, Tentori L (1988) Limb lengthening in achondroplasia by Ilizarov's method. *Int Orthop* 12:173-179.
47. Naski M C, Ornitz D M (1998) FGF signaling in skeletal development. *Front Biosci* 3:d781-794.
48. Krejci P, Masri B, Fontaine V, Mekikian P B, Weis M, Prats H, Wilcox W R (2005) Interaction of fibroblast growth factor and C-natriuretic peptide signaling in regulation of chondrocyte proliferation and extracellular matrix homeostasis. *J Cell Sci* 118:5089-5100.
49. Kake T, Kitamura H, Adachi Y, Yoshioka T, Watanabe T, Matsushita H, Fujii T, Kondo E, Tachibe T, Kawase Y, Jishage K, Yasoda A, Mukoyama M, Nakao K (2009) Chronically elevated plasma C-type natriuretic peptide level stimulates skeletal growth in transgenic mice. *Am J Physiol Endocrinol Metab* 297:E1339-1348.
50. Yasoda A, Kitamura H, Fujii T, Kondo E, Murao N, Miura M, Kanamoto N, Komatsu Y, Arai H, Nakao K (2009) Systemic administration of C-type natriuretic peptide as a novel therapeutic strategy for skeletal dysplasias. *Endocrinology* 150:3138-3144.
51. Igaki T, Itoh H, Suga S I, Hama N, Ogawa Y, Komatsu Y, Yamashita J, Doi K, Chun T H, Nakao K (1998) Effects of intravenously administered C-type natriuretic peptide in humans: comparison with atrial natriuretic peptide. *Hypertens Res* 21:7-13.

Calcif Tissue Int (2012) 90:307–318
DOI 10.1007/s00223-011-9567-0

ORIGINAL RESEARCH

Skeletal Analysis of the Long Bone Abnormality (*lbab/lbab*) Mouse, A Novel Chondrodysplastic C-Type Natriuretic Peptide Mutant

Eri Kondo · Akihiro Yasoda · Takehito Tsuji · Toshihito Fujii · Masako Miura · Naotestu Kanamoto · Naohisa Tamura · Hiroshi Arai · Tetsuo Kunieda · Kazuwa Nakao

Received: 5 July 2011 / Accepted: 22 December 2011 / Published online: 25 January 2012

Abstract Long bone abnormality (*lbab/lbab*) is a strain of dwarf mice. Recent studies revealed that the phenotype is caused by a spontaneous mutation in the *Nppc* gene, which encodes mouse C-type natriuretic peptide (CNP). In this study, we analyzed the chondrodysplastic skeletal phenotype of *lbab/lbab* mice. At birth, *lbab/lbab* mice are only slightly shorter than their wild-type littermates. Nevertheless, *lbab/lbab* mice do not undergo a growth spurt, and their final body and bone lengths are only ~60% of those of wild-type mice. Histological analysis revealed that the growth plate in *lbab/lbab* mice, especially the hypertrophic chondrocyte layer, was significantly thinner than in wild-type mice. Overexpression of CNP in the cartilage of *lbab/lbab* mice restored their thinned growth plate, followed by the complete rescue of their impaired endochondral bone growth. Furthermore, the bone volume in *lbab/lbab* mouse was severely decreased and was recovered by CNP overexpression. On the other hand, the thickness of the growth plate of *lbab/+* mice was not different from that of wild-type mice; accordingly, impaired endochondral bone growth was not observed in *lbab/+* mice. In organ culture experiments, tibial explants from fetal *lbab/lbab* mice were significantly shorter than those from *lbab/+* mice and elongated by addition of 10^{-7} M CNP to the same extent as *lbab/+* tibiae treated with the same dose of CNP. These results demonstrate that *lbab/lbab* is a novel mouse model of chondrodysplasia caused by insufficient CNP action on endochondral ossification.

Keywords C-type natriuretic peptide · Long bone abnormality (*lbab*) · Chondrodysplasia · Endochondral bone growth · Organ culture

C-type natriuretic peptide (CNP) is a member of the natriuretic peptide family and exerts its biological actions through the accumulation of intracellular cyclic GMP via a subtype of membranous guanylyl cyclase receptor, guanylyl cyclase-B (GC-B) [1, 2]. We previously demonstrated that the CNP/GC-B system is a potent stimulator of endochondral bone growth: transgenic mice with targeted overexpression of CNP in cartilage under the control of type II collagen promoter [3] or those with elevated plasma CNP concentrations under the control of human serum amyloid P component promoter [4] exhibit a prominent skeletal overgrowth phenotype. On the other hand, the physiological importance of the CNP/GC-B system on endochondral bone growth has been revealed by the phenotypes of hypomorphs. We generated complete CNP or GC-B null mice and demonstrated that they exhibit an impaired bone growth phenotype [5, 6]. We have also reported that in two lines of spontaneous mutant mice, *cn/cn* and *slw/slw*, disproportionate dwarfism is caused by loss-of-function mutations in the murine GC-B gene [7, 8].

The authors have stated that they have no conflict of interest.

Electronic supplementary material The online version of this article (doi:10.1007/s00223-011-9567-0) contains supplementary material, which is available to authorized users.

E. Kondo · A. Yasoda (✉) · T. Fujii · M. Miura · N. Kanamoto · N. Tamura · H. Arai · K. Nakao
Department of Medicine and Clinical Science, Kyoto University Graduate School of Medicine, Kyoto 606-8507, Japan
e-mail: yasoda@kuhp.kyoto-u.ac.jp

T. Tsuji · T. Kunieda
Department of Animal Science, Okayama University Graduate School of Natural Science and Technology, Okayama 700-8530, Japan

The skeletal phenotypes of these mutant mice resemble those of GC-B knockout mice. Furthermore, recent studies have elucidated that loss-of-function mutations in the human GC-B gene are the causes of acromesomelic dysplasia type Maroteaux (AMDM), one form of skeletal dysplasia with a disproportionate short stature phenotype [9]. The impaired skeletal growth phenotype observed in patients suffering from AMDM is similar to the skeletal phenotype of *cn/cn*, *slw/slw*, and GC-B knockout mice.

The long bone abnormality (*lbab/lbab*) mouse was first identified in The Jackson Laboratory (Bar Harbor, ME) as a spontaneous autosomal recessive mutant characterized by impaired growth of the long bones [10]. Recent studies have elucidated that the impaired growth of *lbab/lbab* mice is caused by a hypomorphic mutation in the CNP gene; Jiao et al. [11] found that its impaired growth phenotype is associated with a single point mutation in the mouse CNP gene, and we showed that this phenotype is completely recovered by CNP overexpression [12]. Yoder et al. [13] characterized the mutant CNP in *lbab/lbab* mice and demonstrated that it is less biologically active than authentic CNP; in whole-cell cGMP elevation and membrane guanylyl cyclase assays, 30-fold to greater than 100-fold more mutant CNP is required to activate GC-B compared to authentic CNP. We also confirmed that the mutant CNP in *lbab/lbab* mice retains only about 10% activity to induce cyclic GMP production through GC-B compared to authentic CNP in an in vitro transfection assay using COS-7 cells [12]. Collectively, *lbab/lbab* is a novel chondrodysplastic mouse model with insufficient CNP action on endochondral bone growth. Nevertheless, the skeletal phenotypes of *lbab/lbab* mice have only been partially described in short reports, including our own brief communication [11–13], and have not yet been fully studied. In this study, we performed further analyses of the skeletal phenotypes of *lbab/lbab* mice.

Materials and Methods

Mice

Heterozygous (*lbab/+*) mice (C57BL/6 J background) were obtained from The Jackson Laboratory, and the strain was maintained by sib mating of heterozygotes. Transgenic mice with targeted overexpression of CNP in the growth plate chondrocytes under the control of the mouse pro-α_1(II) (*Col2a1*) promoter (CNP-Tg) were created as reported previously [3]. To perform genetic rescue of *lbab/lbab* mice, CNP-Tg mice were mated with *lbab/+* mice, and F_1 offspring heterozygous for the transgene and for the *lbab* allele were mated with those with only the *lbab* allele to generate *lbab/lbab* mice with the transgene expression (*lbab/lbab*·CNP-Tg/+ mice) [12]. Genotypes for the CNP transgene and the *lbab* allele were determined by PCR analysis using mouse genomic DNAs extracted from tails. Because there was no tendency of gender differences in the growth of each genotype (data not shown), we used only female mice in our experiments. Animal care and all experiments were conducted in accordance with the Guidelines for Animal Experiments of Kyoto University and were approved by the Animal Research Committee, Graduate School of Medicine, Kyoto University.

Skeletal Analysis

For 10 weeks after birth, body lengths of female mice were measured weekly. Body length was measured as the length from the nose to the anus (nasoanal length) or that from the nose to the tip of the tail (nose–tail length). Body weights were also measured weekly. Skeletal analysis was performed as previously described [14]. Briefly, mice were subjected to soft X-ray analysis (30 kVp, 5 mA for 1 min; Softron type SRO-M5; Softron, Tokyo, Japan), and lengths of the bones were measured on the X-ray films. CT scanning of the humerus was performed using a ScanXmate-L090 Scanner (Comscantechno, Yokohama, Japan). Three-dimensional microstructural image data were reconstructed and structural indices calculated using TRI/3D-BON software (RATOC System Engineering, Tokyo, Japan).

Histological Examination

Tibiae were fixed in 10% formalin neutral buffer, decalcified in 10% EDTA, and embedded in paraffin. Sections (5 μm thick) were sliced and stained with alcian blue (pH 2.5) and hematoxylin–eosin. For immunohistochemistry, sections were incubated with rabbit anti-type X collagen antibody (LSL, Tokyo, Japan), goat anti-Indian hedgehog (Ihh) antibody (Santa Cruz Biotechnology, Santa Cruz, CA), mouse anti-matrix metalloproteinase 13 (MMP-13) antibody (Thermo Fisher Scientific, Waltham, MA), and mouse anti–proliferating cell nuclear antigen (PCNA) antibody (Dako, Copenhagen, Denmark). Immunostaining was performed using the Histofine Mousestain Kit (Nichirei Biosciences, Tokyo, Japan) according to the manufacturer's instruction. Peroxidase activity was visualized using diaminobenzidine. Sections were counterstained with hematoxylin, dehydrated, and then mounted with malinol (Muto Pure Chemicals, Tokyo, Japan). To confirm antibody specificity, normal rabbit serum (Sigma-Aldrich, St. Louis, MO), normal goat IgG (Santa Cruz Biotechnology), and mouse IgG (Dako) were used as first antibodies for negative controls.

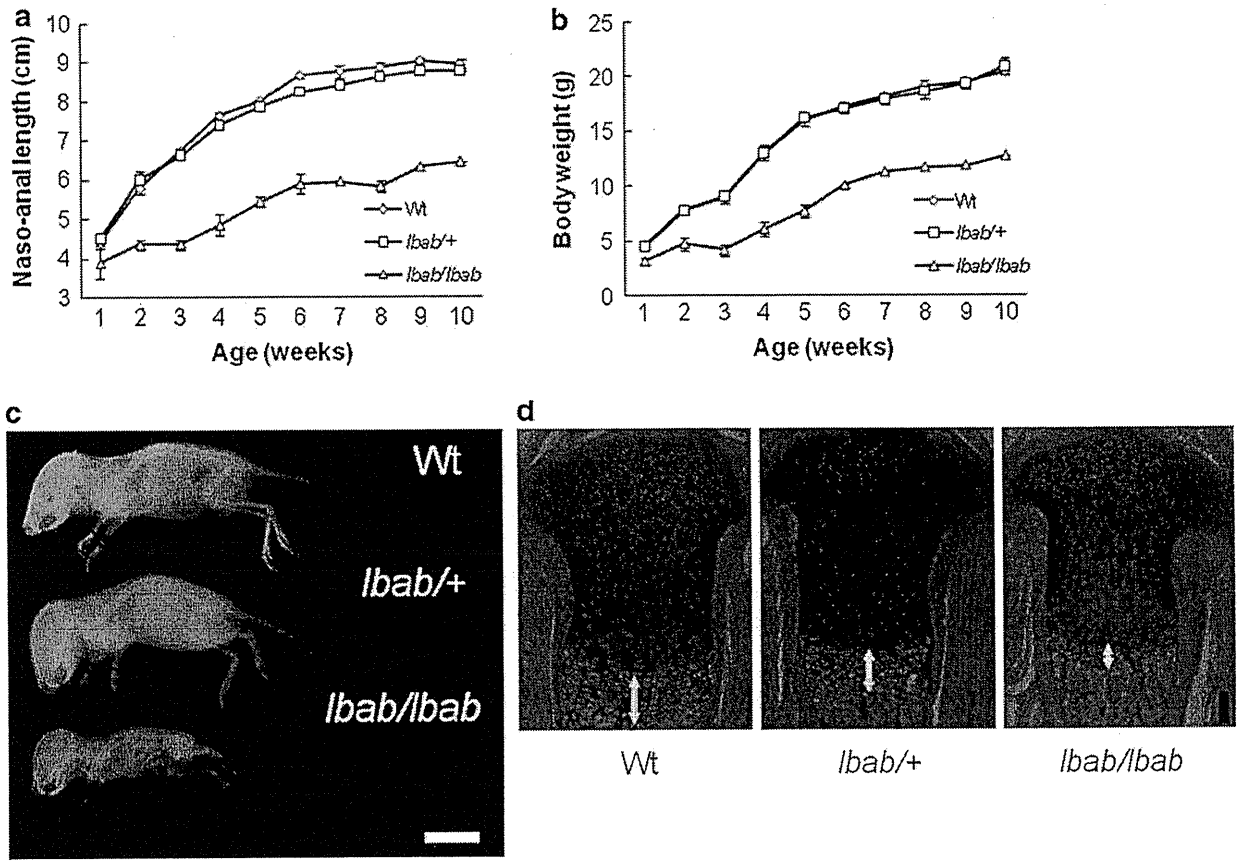

Fig. 1 Growth and skeletal phenotype of *lbab/+* and *lbab/lbab* mice. Nasoanal lengths (**a**) and body weights (**b**) of female wild-type (*Wt, open diamond*), *lbab/+* (*open square*), and *lbab/lbab* (*open triangle*) mice (n = 2–8). **c** Whole skeletons of wild-type, *lbab/+* , and *lbab/lbab* mice at 2 weeks of age. *Scale bar* 1 cm. **d** Histological analysis of the tibial growth plates of 3-day-old mice. *Arrows* indicate hypertrophic chondrocyte layers. Alcian blue and hematoxylin–eosin staining. *Scale bar* 100 μm

Organ Culture

Organ culture of fetal mouse tibiae or third metatarsi was performed as described previously [15]. Tibial or metatarsal explants from *lbab/+* mice and their *lbab/lbab* littermates at 16.5 days postcoitus were cultured for 4 days with vehicle or 10^{-7} M CNP (Peptide Institute, Minoh, Japan). Medium was changed every day. Before and after the culture, the maximal longitudinal lengths of tibiae were measured as the total tibial length, the sum of the lengths of proximal and distal cartilaginous primordia (CP), and the length of the osteogenic center (OC), using a linear ocular scale mounted on an inverted microscope. For histological analysis, explants were fixed in 10% formalin neutral buffer and embedded in paraffin. Sections (5 μm thick) were sliced and stained with alcian blue (pH 2.5) and hematoxylin–eosin. Immunohistochemical staining of incorporated bromodeoxyuridine (BrdU) was performed using 5-Bromo-2′-deoxyuridine labeling and detection kit II (Roche Applied Science, Indianapolis, IN) according to the manufacturer's protocol.

Statistical Analysis

Data were expressed as the mean ± SEM. The statistical significance of differences between mean values was assessed using Student's t-test.

Results

Analyses of Skeletal Growth of *lbab/lbab* and *lbab/+* Mice

As previously reported, *lbab/lbab* mice developed severe dwarfism characterized by short tails and extremities [11, 12]. At birth, *lbab/lbab* pups were slightly shorter than their wild-type littermates: the nasoanal and nose–tail lengths of *lbab/lbab* mice were 88 and 83% of those of

their wild-type littermates, respectively (Fig. 1a, Supplemental Fig. 1).The ratios of nasoanal and nose–tail lengths of *lbab/lbab* mice to those of wild-type mice sharply decreased to 65% and 55%, respectively, by the age of 3 weeks. After 5 weeks of age, these ratios stabilized at 66–72% and 57–62%, respectively (Fig. 1a, Supplemental Fig. 1). The body weight of *lbab/lbab* mice was 68% of that of their wild-type littermates at birth and decreased to 46% by the age of 3 weeks. The ratio did not increase until 5 weeks of age, becoming ~60% after 7 weeks (Fig. 1b). On the other hand, *lbab/+* mice were indistinguishable from their wild-type littermates at birth and grew almost similarly (Fig. 1a,b, Supplemental Fig. 1). Soft X-ray analysis revealed that longitudinal growth of the vertebrae, tail, and extremities was affected in *lbab/lbab* mice at the age of 2 weeks but was not affected in *lbab/+* mice (Fig. 1c). Histological analysis revealed that at the age of 3 days the tibial growth plate, especially the hypertrophic chondrocyte layer, of *lbab/lbab* mice was apparently thinner than that of wild-type mice (Fig. 1d). On the other hand, the thickness of the tibial growth plate of *lbab/+* mice was not different from that of wild-type mice (Fig. 1d).

Effect of CNP Overexpression on Impaired Endochondral Bone Growth of *lbab/lbab* Mice

In order to further characterize the impaired skeletal growth of *lbab/lbab* mice, we analyzed how their impaired endochondral bone growth recovered in response to targeted overexpression of CNP in the cartilage in vivo [12]. We crossed *lbab/lbab* mice with cartilage-specific CNP transgenic mice under the control of type II collagen promoter (CNP-Tg mice) and obtained *lbab/lbab* mice with transgenic expression of CNP in cartilage (*lbab/lbab*·CNP-Tg mice) [12]. At the first week after birth, the nasoanal length of *lbab/lbab*·CNP-Tg mice was almost the same as that of *lbab/lbab* mice and considerably smaller than that of wild-type mice: nasoanal lengths of wild-type, *lbab/lbab*, and *lbab/lbab*·CNP-Tg mice were 4.38 ± 0.06, 3.87 ± 0.37, and 4.00 ± 0.12 cm, respectively. Subsequently, *lbab/lbab*·CNP-Tg mice began to grow larger than *lbab/lbab* mice and promptly caught up with wild-type mice; although the nasoanal length of *lbab/lbab*·CNP-Tg mice was still considerably smaller than that of wild-type mice until 3 weeks of age (5.70 ± 0.57 and 6.71 ± 0.10 cm, respectively, at age 3 weeks), it became almost comparable to that of wild-type mice after 4 weeks (7.38 ± 0.48 and 7.61 ± 0.10 cm, respectively, at age 4 weeks). Further, the body weight of *lbab/lbab*·CNP-Tg mice was almost the same as that of *lbab/lbab* mice and smaller than that of wild-type mice until the age of 3 weeks but then promptly increased to a level comparable to that of wild-type mice (Supplemental Fig. 2).

Soft X-ray analyses revealed that at the age of 2 weeks the impaired growth of bones formed through endochondral ossification in *lbab/lbab* mice was partially recovered by targeted overexpression of CNP in cartilage in *lbab/lbab*·CNP-Tg mice (Fig. 2a): the recoveries in the longitudinal length of cranium and the lengths of the humerus, radius, ulna, femur, tibia, and vertebrae were 35, 73, 68, 37, 51, 63, and 27%, respectively (Fig. 2b). Furthermore, at the age of 10 weeks, the impaired endochondral bone growth in *lbab/lbab* mice was almost completely recovered by targeted overexpression of CNP in cartilage, as observed in *lbab/lbab*·CNP-Tg mice (Fig. 2c, d). On the other hand, there were no significant differences in the width of the cranium, which is formed via intramembranous ossification, among the three genotypes at either 2 or 10 weeks (Fig. 2b, d).

Histological analysis showed that the thickness of both the proliferative chondrocyte layer and the hypertrophic chondrocyte layer, positive for immunohistochemical staining for type X collagen, was significantly decreased in *lbab/lbab* mice compared to wild-type mice at the age of 2 weeks, as previously reported [12] (Fig. 3a, b).The thinner proliferative chondrocyte layer in the *lbab/lbab* growth plate was completely recovered by targeted overexpression of CNP as observed in the *lbab/lbab*·CNP-Tg growth plate (Fig. 3c). The thinner hypertrophic chondrocyte layer in the *lbab/lbab* growth plate was also considerably recovered in the *lbab/lbab*·CNP-Tg growth plate, although the extent of the recovery was less than in the proliferative chondrocyte layer (Fig. 3d). Immunohistochemical staining for PCNA revealed that the number of PCNA-positive cells was severely decreased in the proliferative chondrocyte layer of the *lbab/lbab* growth plate (Fig. 3e). The number of PCNA-positive cells did not recover in the proliferative chondrocyte layer of the *lbab/lbab*·CNP-Tg growth plate, whereas the thinner proliferative chondrocyte layer in the *lbab/lbab* growth plate was almost completely recovered in the *lbab/lbab*·CNP-Tg growth plate (Fig. 3c). The area positive for immunostaining of Ihh, one of the markers of hypertrophic differentiation, was decreased in the *lbab/lbab* growth plate compared to the wild-type growth plate (Fig. 3f). The smaller size of the area positive for Ihh in the *lbab/lbab* growth plate was almost completely recovered in the *lbab/lbab*·CNP-Tg growth plate (Fig. 3f). Immunohistochemical staining of MMP-13, a useful marker for terminal hypertrophic chondrocytes, was not changed between the three genotypes, indicating that the progression through the hypertrophy program was not accelerated in the *lbab/lbab* growth plate (Fig. 3g).

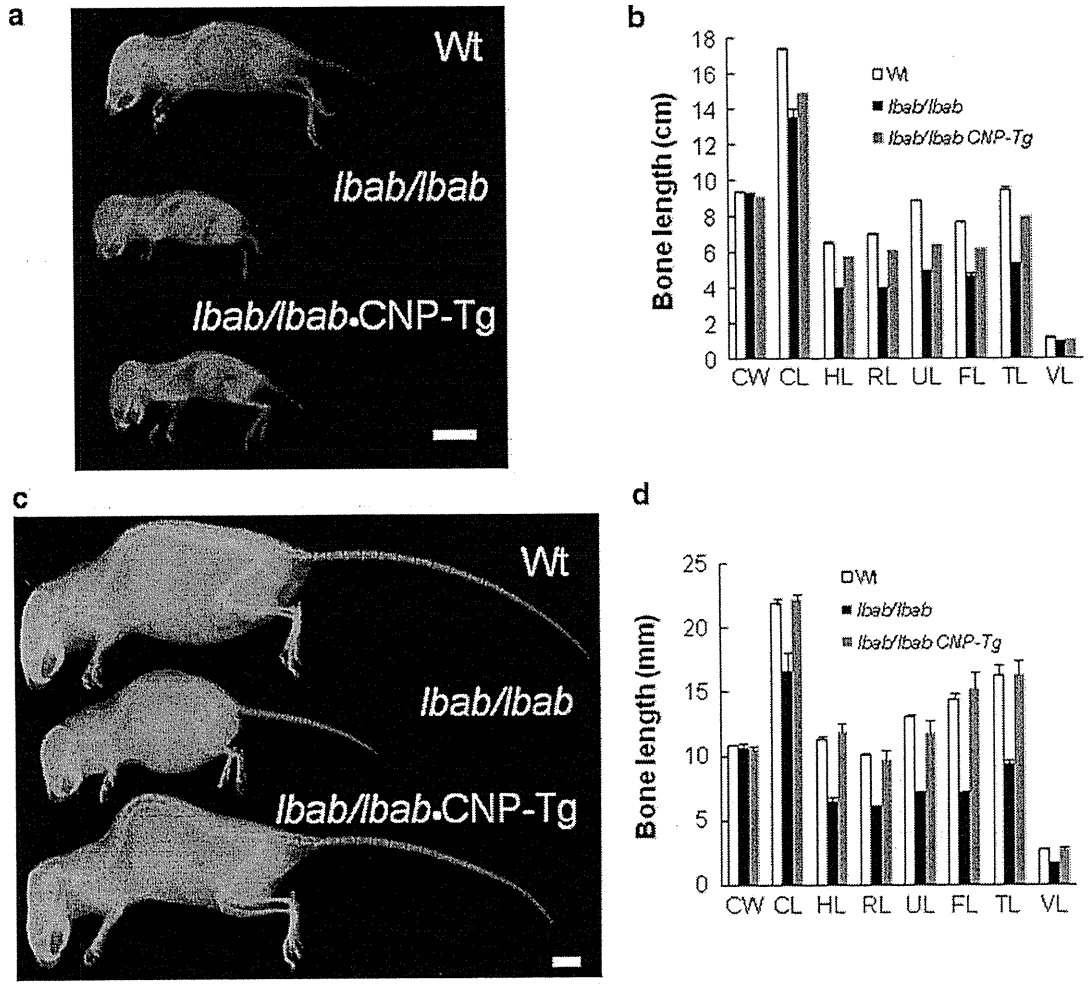

Fig. 2 Effect of CNP overexpression on impaired endochondral bone growth of *lbab/lbab* mice. Whole skeletons (**a**, **c**) and bone lengths measured on soft X-ray films (**b**, **d**) of female wild-type (*Wt*), *lbab/lbab*, and *lbab/lbab*·CNP-Tg mice at the age of 2 weeks (**a**, **b**) and 10 weeks (**c**, **d**). **a**, **c** *Scale bar* 1 cm. **b**, **d** *White bars*, wild-type mice; *black bars*, *lbab/lbab* mice; *gray bars*, *lbab/lbab*·CNP-Tg mice. *CW*, width of cranium; *CL*, longitudinal length of cranium; *HL*, humeral length; *RL*, radial length; *UL*, ulnar length; *FL*, femoral length; *TL*, tibial length; *VL*, vertebral length. $n = 2$–7 (**b**) and 3–5 (**d**) (Color figure online)

At the age of 10 weeks, the tibial growth plate of *lbab/lbab* mice continued to be thinner than that of wild-type mice and was completely recovered by overexpression of CNP in cartilage (Fig. 4).

Recovery of Decreased Bone Volume in *lbab/lbab* Mouse by CNP Overexpression

Three-dimensional CT analysis manifested a marked reduction in bone volume of the humerus in *lbab/lbab* mice and considerable recovery in *lbab/lbab*·CNP-Tg mice (Fig. 5). At the age of 10 weeks, the quantified bone volume (BV/TV) and trabecular thickness (Tb.Th) of the humerus in *lbab/lbab* mice were 2.4% and 34.5 μm, whereas those in wild-type mice were 4.1% and 40.3 μm, respectively. The decreased BV/TV and Tb.Th in *lbab/lbab* mice were increased to 5.4% and 37.0 μm, respectively, in *lbab/lbab*·CNP-Tg mice.

Organ Culture Experiments of Tibiae from *lbab/lbab* Mice

In order to further analyze the impaired endochondral ossification of *lbab/lbab* mice, we preformed organ culture experiments using tibial explants from fetal mice (Fig. 6a) [15]. Because skeletal phenotypes of mice heterozygous for the *lbab* allele were not different from those of wild-type mice, we compared the growth of tibial explants from *lbab/lbab* mice with that from *lbab/+* mice. At the beginning of culture, both the total length and the sum length of the CP of *lbab/lbab* tibiae were significantly smaller than those of *lbab/+* tibiae (3.80 ± 0.04

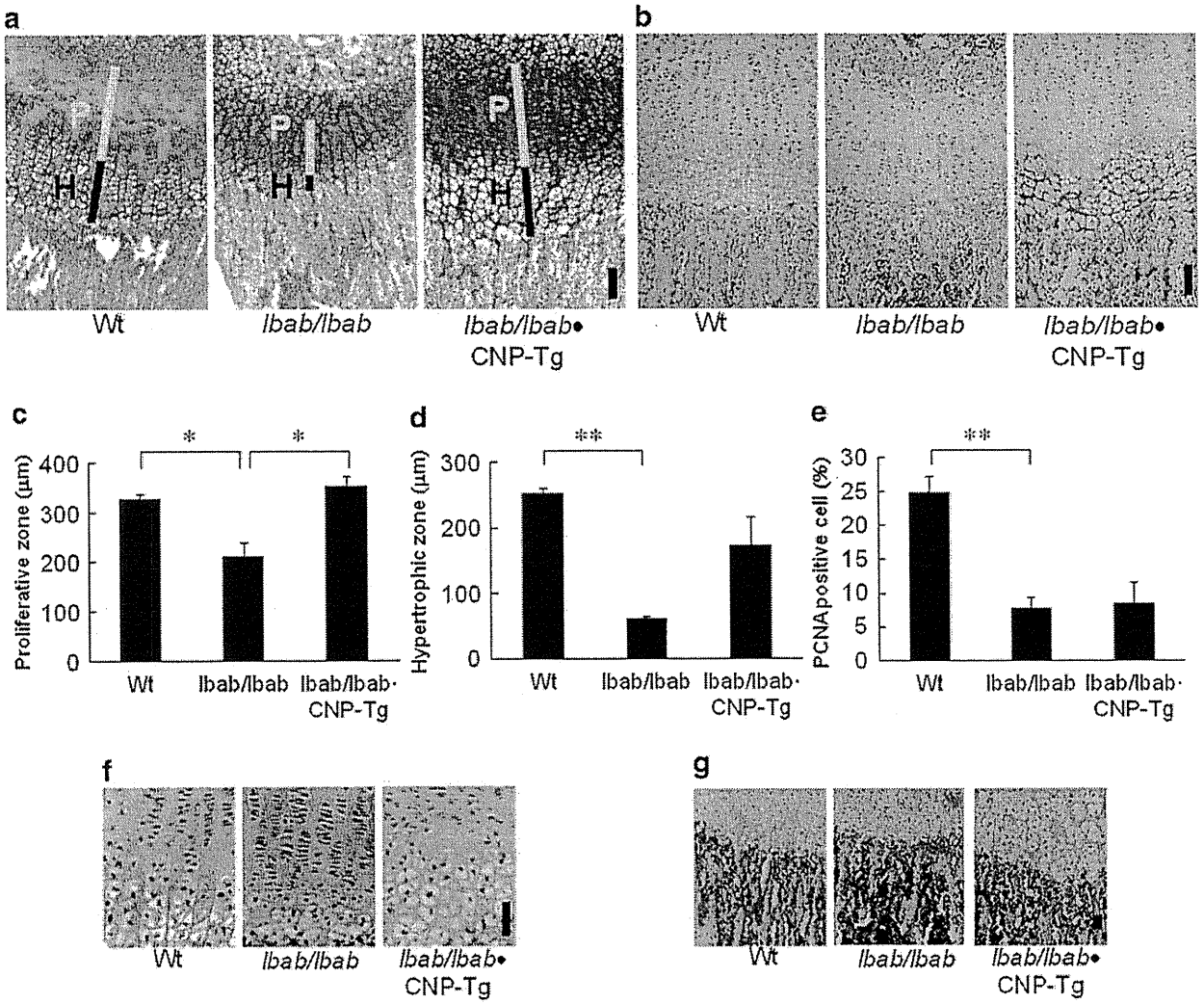

Fig. 3 Histological analysis of tibial growth plates from 2-week-old wild-type (*Wt*), *lbab/lbab*, and *lbab/lbab*·CNP-Tg mice. **a** Alcian blue and hematoxylin–eosin staining. *Yellow bars* (depicted as *P*) indicate proliferative chondrocyte layers, and *red bars* (depicted as *H*) indicate hypertrophic chondrocyte layers. **b** Immunohistochemical staining for type X collagen. Scale bar in **a** and **b** = 100 μm. Heights of the proliferative (**c**) and hypertrophic (**d**) chondrocyte layers. $n = 3$ each. $^{*}P < 0.05$, $^{**}P < 0.01$. **e** The proportion of PCNA-positive chondrocytes in proliferative chondrocyte layers. $n = 3$–4. $^{**}P < 0.01$. Immunohistochemical staining of Ihh (**f**) and MMP-13 (**g**). Scale bar in **f** and **g** = 50 μm

vs. 4.25 ± 0.03 and 2.19 ± 0.02 vs. 2.43 ± 0.01 mm, respectively, $n = 8$–12 each) (Fig. 6b, c). Tibial explants from *lbab/lbab* mice grew to the same extent as those from *lbab/+* mice during a 4-day culture period; the difference in the total length or in the length of the CP between *lbab/lbab* and *lbab/+* explants at the end of culture was comparable to that at the beginning of culture (Fig. 6b, c). There was no significant difference in the length of the OC between the two genotypes before and after the culture period (data not shown).

The treatment of CNP at the dose of 10^{-7} M stimulated the growth of both *lbab/lbab* and *lbab/+* tibiae (Fig. 6b, c). CNP stimulated the growth of *lbab/lbab* tibiae more potently than that of *lbab/+* tibiae; in the presence of 10^{-7} M CNP, the difference between the total length of *lbab/+* tibiae and that of *lbab/lbab* tibiae was decreased (Fig. 6b), and furthermore, the CP length of *lbab/lbab* tibiae became almost the same as that of *lbab/+* tibiae (Fig. 6c). The growth of the OC was not stimulated by CNP in either *lbab/lbab* or *lbab/+* explants (data not shown).

Histological examination at the end of the culture period revealed that the length of the primordial growth plate (Fig. 7a), especially that of the hypertrophic chondrocyte layer positive for type X collagen immunostaining (Fig. 7b,c), was smaller in *lbab/lbab* explants than in

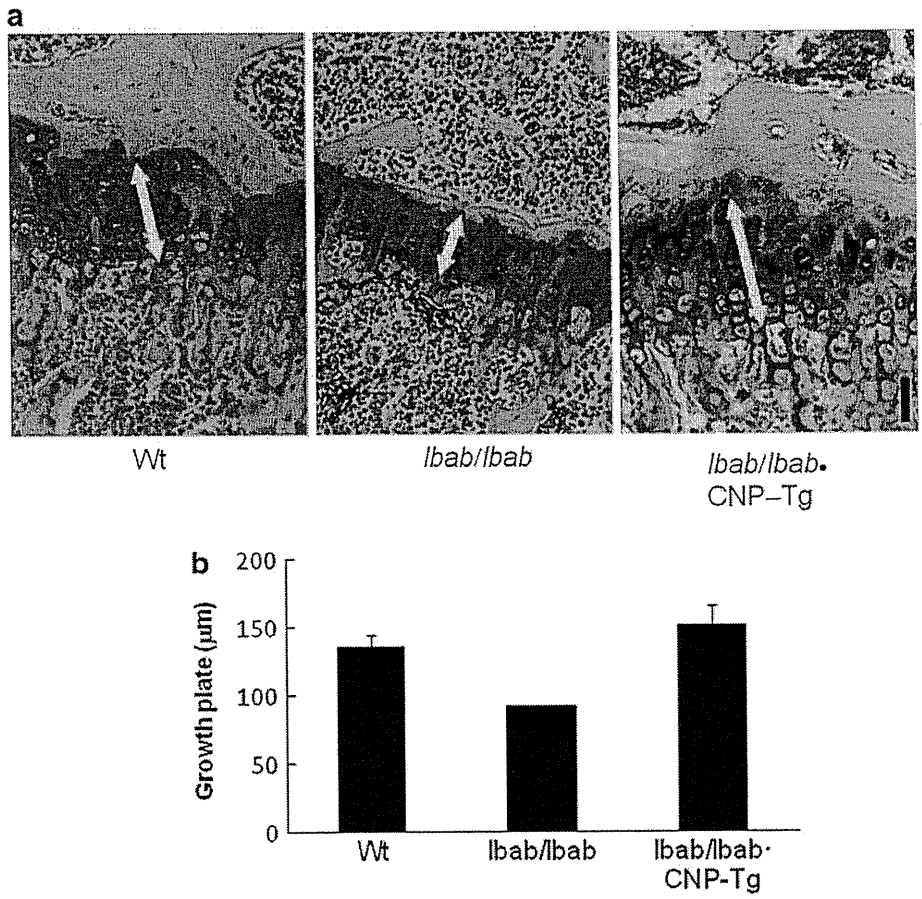

Fig. 4 Histological analysis of tibial growth plate from female 10-week-old wild-type (*Wt*), *lbab/lbab*, and *lbab/lbab*·CNP-Tg mice. **a** Alcian blue and hematoxylin–eosin staining. *Arrows* indicate the width of growth plates. *Scale bar* 50 μm. **b** Total heights of the growth plates. $n = 2$–5 each

lbab/+ explants. The area positive for immunostaining for Ihh, one of the markers for chondrogenic differentiation [16], tended to be a little decreased in *lbab/lbab* explants compared to that in *lbab/+* explants, although the intensity of the immunostaining was not different between the two genotypes (Supplemental Fig. 3). Immunohistochemical detection of BrdU-incorporated chondrocytes revealed that BrdU-positive chondrocytes tended to be decreased in *lbab/lbab* explants compared to those in *lbab/+* explants (Fig. 7d). Addition of CNP prominently increased the lengths of primordial growth plates (Fig. 7a) and their hypertrophic chondrocyte layers (Fig. 7b, c) of both *lbab/+* and *lbab/lbab* explants. The lengths of the primordial growth plate and its hypertrophic chondrocyte layer of *lbab/lbab* explants treated with 10^{-7} M CNP became comparable to those of *lbab/+* explants treated with the same dose of CNP (Fig. 7a–c). CNP increased the areas positive for Ihh immunostaining in both *lbab/+* and *lbab/lbab* explants. By addition of CNP, the sizes of the areas positive for, and the intensities of, Ihh immunostaining were not different between *lbab/+* and *lbab/lbab* explants (Supplemental Fig. 3). CNP did not increase BrdU-positive chondrocytes in *lbab/lbab* explants (Fig. 7d).

Further, we explored whether CNP controls the progression of growth plate chondrocytes through the different stages of maturation or not. Because the process of endochondral ossification is delayed in the metatarsus compared to that in the tibia in an individual, we performed organ culture of metatarsi as well as tibiae from fetal mice at 16.5-days postcoitus and examined the expression of type X collagen and Ihh. In the case of *lbab/+* organ culture, the area positive for immunostaining of type X collagen was reduced and that of Ihh was localized near the ossification center in metatarsal explants compared with those in tibial explants, indicating that the metatarsal growth plate represents an earlier stage of endochondral ossification than the tibial growth plate (Fig. 8). The area positive for immunostaining of type X collagen was greatly reduced in *lbab/lbab* metatarsal explants compared with that in *lbab/+* metatarsal explants and recovered by addition of 10^{-7} M CNP to the same extent to that in *lbab/+* metatarsal explants treated with vehicle. The area positive for immunostaining of Ihh became closer to ossification center

Fig. 5 Micro-CT analysis of humeri from wild-type (*Wt*), *lbab/lbab*, and *lbab/lbab*·CNP-Tg mice at the age of 10 weeks. *Scale bar* 1 mm

in *lbab/lbab* metatarsal explants than in *lbab/+* metatarsal explants and was returned to the same position as *lbab/+* metatarsal explants by addition of CNP (Fig. 8).

Discussion

Previously, we and other groups had reported in brief communications that the short stature phenotype of *lbab/lbab* mice is caused by a mutation in the CNP gene [11–13]. Here, we further analyzed the skeletal phenotypes of *lbab/lbab* mice and report the results in this full-length article.

Analysis of the growth curves of nasoanal and nose–tail lengths revealed that the shortness of *lbab/lbab* mice is mild at birth but rapidly progresses by the age of 3 weeks, and then, after 4 weeks, the ratio of the length of *lbab/lbab* mice compared to that of wild-type mice becomes almost constant. This suggests that CNP is especially crucial for the skeletal growth spurt that occurs in early life. Since CNP is expressed in the growth plate cartilage and works as an autocrine/paracrine regulator [5], CNP might affect the endochondral bone growth potently when the volume of growth plate cartilage is relatively abundant.

We confirmed the thinness of the growth plate of *lbab/lbab* mice, especially in its hypertrophic chondrocyte layer, followed by the impaired growth of long bones. The thinness of the growth plate of *lbab/lbab* mice was almost completely recovered by targeted overexpression of CNP in the growth plate by the age of 2 weeks. On the other hand, the recovery of the shortness of the total length of *lbab/lbab* bones by CNP was only partial at 2 weeks, becoming complete at the age of 10 weeks. This finding suggests that the recovery is evident earlier in the thickness of the growth plate than in the total bone length. In addition, immunohistochemistry for PCNA revealed that at the age of 2 weeks the proliferation of growth plate chondrocytes is decreased in *lbab/lbab* mice and that the decreased proliferation is not rescued by CNP overexpression, even though the thickness of the growth plate does fully recover.

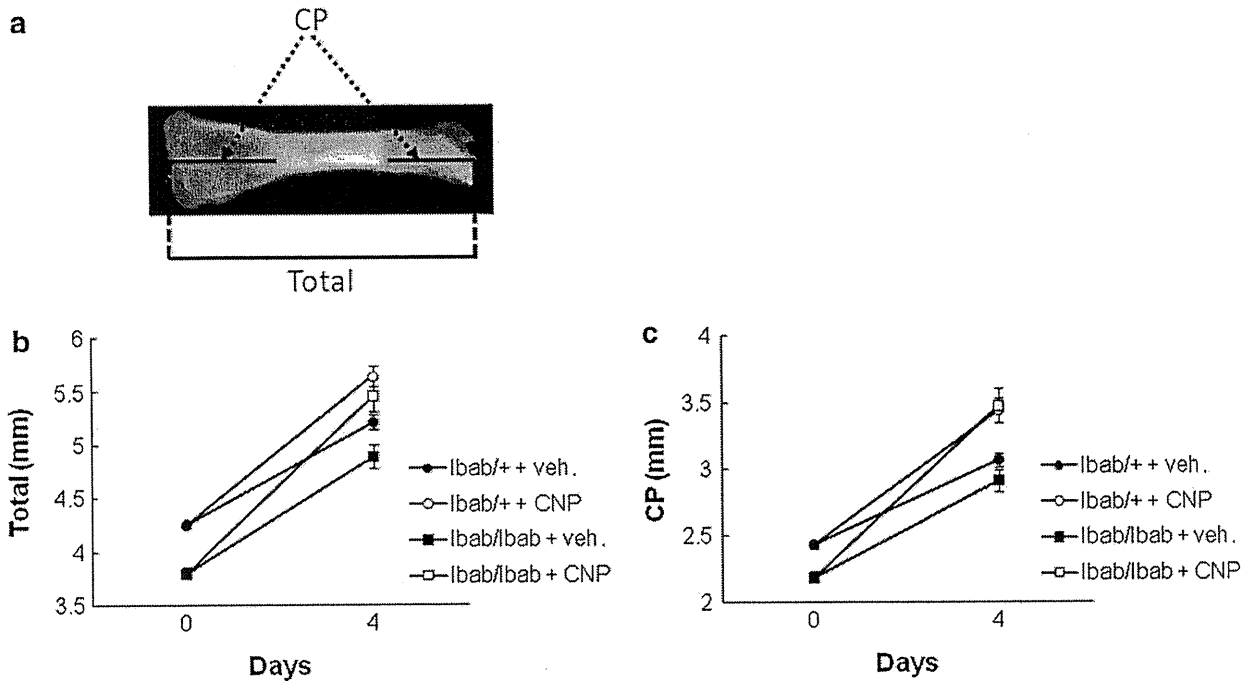

Fig. 6 Effect of CNP on cultured tibiae from fetal *lbab/+* and *lbab/lbab* mice. **a** A representative picture of a tibial explant from a fetal mouse. Total longitudinal length (*Total*) and the sum lengths of cartilaginous primordia (*CP*) are indicated. Graphs of total (**b**) and CP (**c**) lengths of cultured tibiae from *lbab/+* and *lbab/lbab* mice treated with vehicle (*veh.*) or 10^{-7} M CNP (*CNP*) for 4 days. *Circles* indicate *lbab/+* tibiae, and *squares* indicate *lbab/lbab* tibiae. At the end of culture, *closed symbols* indicate tibiae treated with vehicle and *open symbols* indicate those treated with CNP. $n = 8$–12 each

The reason the decreased proliferation of chondrocytes in the *lbab/lbab* growth plate was not rescued by CNP overexpression in chondrocytes is not clear, but it may be because of the weak and slow expression of the CNP transgene owing to the weak power of the promoter region. On the other hand, CNP could not increase the proliferation of growth plate chondrocytes in *lbab/lbab* explants in organ culture experiments in this study. The effect of CNP on chondrocyte proliferation might be so mild that other effects of CNP on growth plate chondrocytes, e.g., the stimulatory effect on matrix synthesis as we had previously reported [3, 4], might proceed to recover the thinned growth plate of *lbab/lbab* mice. The discrepancy between the effects on proliferation and matrix synthesis may explain in part the delayed recovery of bone length relative to growth plate thickness. On the other hand, immunohistochemical staining of type X collagen and Ihh in explanted growth plates at two different stages of endochondral ossification suggested that the progression of proliferative chondrocytes to hypertrophic chondrocytes was delayed in the *lbab/lbab* growth plate and recovered by addition of CNP. In addition to the result that the expression of MMP-13 was not different between the terminal hypertrophic chondrocytes of wild-type, *lbab/lbab*, and rescued growth plates, CNP might promote the hypertrophic differentiation of proliferative chondrocytes but not accelerate the terminal differentiation of hypertrophic chondrocytes.

In this study, we investigated the character of calcified bones of *lbab/lbab* mice using three-dimensional CT analysis: the bone volume of *lbab/lbab* mice was substantially decreased compared to that of wild-type mice and recovered by cartilage-specific CNP overexpression. The mechanism of decrease in bone volume of *lbab/lbab* mice is still unknown, but CNP may be expressed in and affect cells other than chondrocytes, i.e., osteoblasts or osteoclasts, in bone. Although overexpression of CNP was targeted to chondrocytes in our rescue experiments, early onset of CNP-Tg expression from the CP might have been able to affect bone metabolism at the earlier stage of skeletogenesis [17] and may have continued to affect osteoblasts or osteoclasts near the growth plate cartilage in the later stage of skeletogenesis. Whereas several in vitro effects of CNP on osteoblastic cell lineages or osteoclasts have been reported [18–28], the in vivo effects of CNP on bone metabolism remain elusive; and further experiments are now ongoing in our laboratory.

We previously discovered that in two strains of mice, *cn/cn* and *slw/slw*, dwarfism is caused by spontaneous

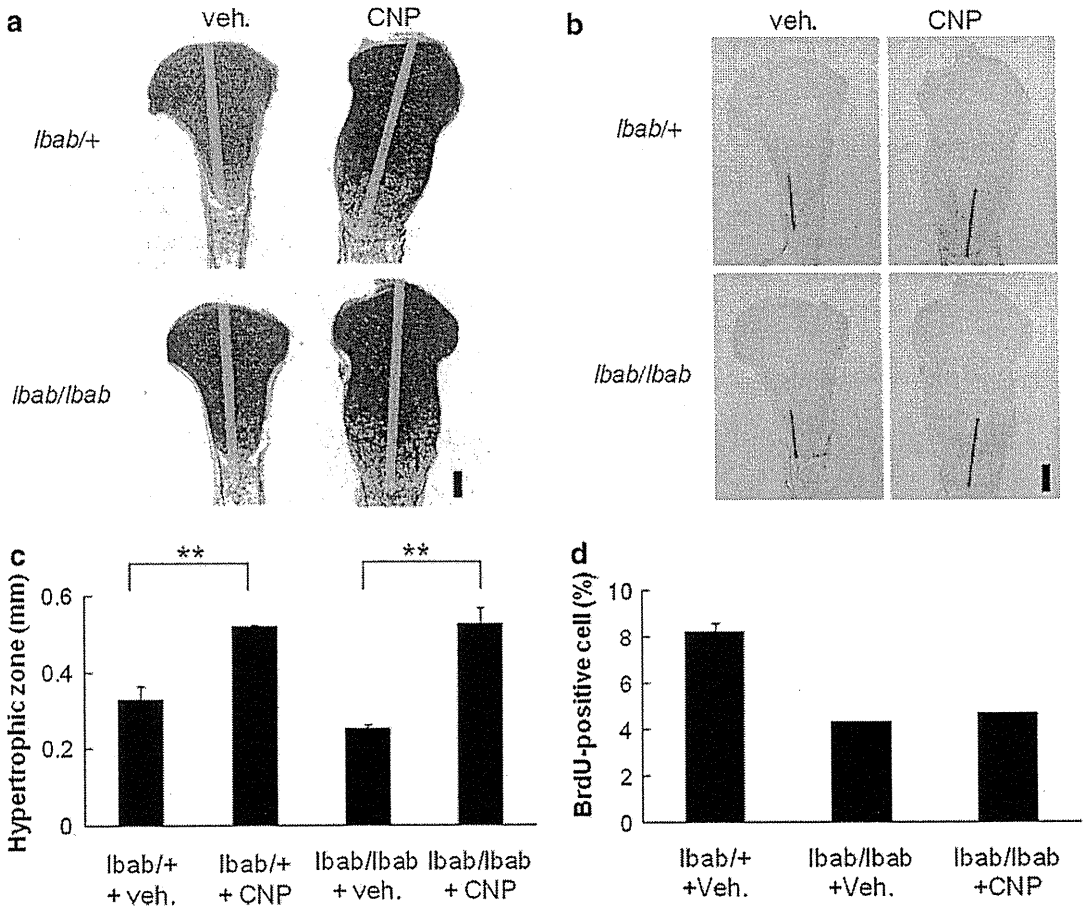

Fig. 7 Histological analyses of the growth plates of tibial explants from fetal *lbab/+* and *lbab/lbab* mice treated with vehicle (*veh.*) or 10^{-7} M CNP (*CNP*) for 4 days. Alcian blue and hematoxylin–eosin staining (**a**) and immunohistochemical staining for type X collagen (**b**). *Yellow bars* in **a** indicate lengths of cartilaginous primordial, and *red bars* in **b** indicate heights of hypertrophic chondrocyte layers. *Scale bars* 200 μm. Height of hypertrophic chondrocyte layer (**c**) and proportion of BrdU-positive cells (**d**) of the growth plate of tibial explant from fetal *lbab/+* or *lbab/lbab* mice treated with 10^{-7} M CNP or vehicle at the end of the 4-day culture period. $n = 3$ each. $^{**}P < 0.01$ in **c** and $n = 2$–3 each in **d** (Color figure online)

mutations in the GC-B gene [7, 8]. In humans, it has been identified that AMDM is caused by spontaneous loss-of-function mutations in the GC-B gene [9, 29]. The *lbab/lbab* mouse, the skeletal phenotype of which we have closely analyzed in the present report, has a spontaneous loss-of-function mutation in the CNP gene; by analogy to the GC-B gene, some forms of human skeletal dysplasia might be caused by mutations in the CNP gene. Thus far, no such conditions have been discovered [30]. In the event such a discovery is made, the *lbab/lbab* mouse would then be a novel model of a form of human skeletal dysplasia caused by a mutation in the CNP gene.

In contrast to mice homozygous for the *lbab* allele, the growth and skeletal phenotype of mice heterozygous for the *lbab* allele were not different from those of wild-type mice, as is the case with heterozygous CNP knockout mice. This confirms that haploinsufficiency for the CNP gene does not exist in mice. Likewise, heterozygotes for the GC-B knockout, the *cn* allele, or the *slw* allele exhibit no skeletal abnormalities [6–8]; thus, haploinsufficiency of the GC-B gene also does not exist in mice. Nevertheless, haploinsufficiency of the GC-B gene does exist in humans: heterozygous carriers of AMDM are reported to be shorter than expected for their population of origin [31]. The reason for the discrepancy is not clear at present, but it may have to do with differences between species or some other unknown mechanism(s). We will have to perform further investigations on the skeletal phenotypes of the aforementioned lines of GC-B mutant mice; such experiments are now ongoing in our laboratory.

In summary, in this study we more closely investigated the skeletal phenotypes of a novel CNP mutant mouse, *lbab/lbab*. The results of this study will be useful not only for further elucidation of the physiological role of CNP on

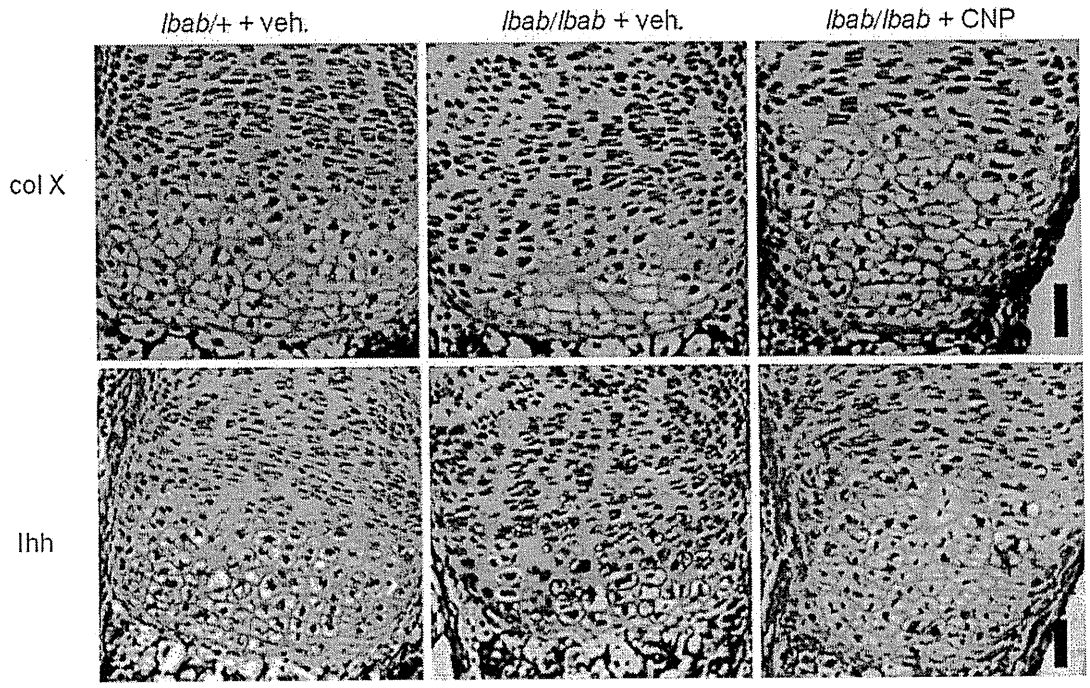

Fig. 8 Immunohistochemical staining of type X collagen (*upper panels*) and Ihh (*lower panels*) of the growth plates of metatarsal explants from fetal *lbab/+* and *lbab/lbab* mice treated with vehicle (*veh.*) or 10^{-7} M CNP for 4 days. *Scale bar* 50 μm

endochondral bone growth but also for the prediction of pathophysiology of a hypothetical chondrodysplasia caused by a mutation in the human CNP gene, which has not yet been discovered.

Acknowledgments We thank B. de Crombrugghe (Department of Genetics, University of Texas M.D. Anderson Cancer Center) for the *Col2a1* promoter. This study was supported by a Grant-in-Aid for Scientific Research from the Ministry of Health, Labor, and Welfare of Japan and the Ministry of Education, Culture, Sports, Sciences, and Technology of Japan (21591176, 21119013).

References

1. Nakao K, Ogawa Y, Suga S, Imura H (1992) Molecular biology and biochemistry of the natriuretic peptide system. I: Natriuretic peptides. J Hypertens 10:907–912
2. Nakao K, Ogawa Y, Suga S, Imura H (1992) Molecular biology and biochemistry of the natriuretic peptide system. II: Natriuretic peptide receptors. J Hypertens 10:1111–1114
3. Yasoda A, Komatsu Y, Chusho H, Miyazawa T, Ozasa A, Miura M, Kurihara T, Rogi T, Tanaka S, Suda M, Tamura N, Ogawa Y, Nakao K (2004) Overexpression of CNP in chondrocytes rescues achondroplasia through a MAPK-dependent pathway. Nat Med 10:80–86
4. Kake T, Kitamura H, Adachi Y, Yoshioka T, Watanabe T, Matsushita H, Fujii T, Kondo E, Tachibe T, Kawase Y, Jishage K, Yasoda A, Mukoyama M, Nakao K (2009) Chronically elevated plasma C-type natriuretic peptide level stimulates skeletal growth in transgenic mice. Am J Physiol Endocrinol Metab 297:E1339–E1348
5. Chusho H, Tamura N, Ogawa Y, Yasoda A, Suda M, Miyazawa T, Nakamura K, Nakao K, Kurihara T, Komatsu Y, Itoh H, Tanaka K, Saito Y, Katsuki M, Nakao K (2001) Dwarfism and early death in mice lacking C-type natriuretic peptide. Proc Natl Acad Sci USA 98:4016–4021
6. Tamura N, Doolittle LK, Hammer RE, Shelton JM, Richardson JA, Garbers DL (2004) Critical roles of the guanylyl cyclase B receptor in endochondral ossification and development of female reproductive organs. Proc Natl Acad Sci USA 101:17300–17305
7. Tsuji T, Kunieda T (2005) A loss-of-function mutation in natriuretic peptide receptor 2 (*Npr2*) gene is responsible for disproportionate dwarfism in *cn/cn* mouse. J Biol Chem 280: 14288–14292
8. Sogawa C, Tsuji T, Shinkai Y, Katayama K, Kunieda T (2007) Short-limbed dwarfism: *slw* is a new allele of Npr2 causing chondrodysplasia. J Hered 98:575–580
9. Bartels CF, Bükülmez H, Padayatti P, Rhee DK, van Ravenswaaij-Arts C, Pauli RM, Mundlos S, Chitayat D, Shih LY, Al-Gazali LI, Kant S, Cole T, Morton J, Cormier-Daire V, Faivre L, Lees M, Kirk J, Mortier GR, Leroy J, Zabel B, Kim CA, Crow Y, Braverman NE, van den Akker F, Warman ML (2004) Mutations in the transmembrane natriuretic peptide receptor NPR-B impair skeletal growth and cause acromesomelic dysplasia, type Maroteaux. Am J Hum Genet 75:27–34
10. The Jackson Laboratory. http://www.jax.org/index.html
11. Jiao Y, Yan J, Jiao F, Yang H, Donahue LR, Li X, Roe BA, Stuart J, Gu W (2007) A single nucleotide mutation in Nppc is associated with a long bone abnormality in *lbab* mice. BMC Genet 8:16
12. Tsuji T, Kondo E, Yasoda A, Inamoto M, Kiyosu C, Nakao K, Kunieda T (2008) Hypomorphic mutation in mouse *Nppc* gene

causes retarded bone growth due to impaired endochondral ossification. Biochem Biophys Res Commun 376:186–190
13. Yoder AR, Kruse AC, Earhart CA, Ohlendorf DH, Potter LR (2008) Reduced ability of C-type natriuretic peptide (CNP) to activate natriuretic peptide receptor B (NPR-B) causes dwarfism in *lbab-/-* mice. Peptides 29:1575–1581
14. Suda M, Ogawa Y, Tanaka K, Tamura N, Yasoda A, Takigawa T, Uehira M, Nishimoto H, Itoh H, Saito Y, Shiota K, Nakao K (1998) Skeletal overgrowth in transgenic mice that overexpress brain natriuretic peptide. Proc Natl Acad Sci USA 95:2337–2342
15. Yasoda A, Ogawa Y, Suda M, Tamura N, Mori K, Sakuma Y, Chusho H, Shiota K, Tanaka K, Nakao K (1998) Natriuretic peptide regulation of endochondral ossification. Evidence for possible roles of the C-type natriuretic peptide/guanylyl cyclase-B pathway. J Biol Chem 273:11695–11700
16. Vortkamp A, Lee K, Lanske B, Segre GV, Kronenberg HM, Tabin CJ (1996) Regulation of rate of cartilage differentiation by Indian hedgehog and PTH-related protein. Science 273:613–622
17. Zhou G, Garofalo S, Mukhopadhyay K, Lefebvre V, Smith CN, Eberspaecher H, de Crombrugghe B (1995) A 182 bp fragment of the mouse pro alpha 1(II) collagen gene is sufficient to direct chondrocyte expression in transgenic mice. J Cell Sci 108(Pt 12): 3677–3684
18. Inoue A, Hiruma Y, Hirose S, Yamaguchi A, Furuya M, Tanaka S, Hagiwara H (1996) Stimulation by C-type natriuretic peptide of the differentiation of clonal osteoblastic MC3T3-E1 cells. Biochem Biophys Res Commun 221:703–707
19. Hagiwara H, Inoue A, Yamaguchi A, Yokose S, Furuya M, Tanaka S, Hirose S (1996) cGMP produced in response to ANP and CNP regulates proliferation and differentiation of osteoblastic cells. Am J Physiol Cell Physiol 270:C1311–C1318
20. Suda M, Tanaka K, Fukushima M, Natsui K, Yasoda A, Komatsu Y, Ogawa Y, Itoh H, Nakao K (1996) C-type natriuretic peptide as an autocrine/paracrine regulator of osteoblast. Evidence for possible presence of bone natriuretic peptide system. Biochem Biophys Res Commun 223:1–6
21. Yanaka N, Akatsuka H, Kawai E, Omori K (1998) 1,25-Dihydroxyvitamin D_3 upregulates natriuretic peptide receptor-C expression in mouse osteoblasts. Am J Physiol Endocrinol Metab 275:E965–E973
22. Inoue A, Hayakawa T, Otsuka E, Kamiya A, Suzuki Y, Hirose S, Hagiwara H (1999) Correlation between induction of expression of biglycan and mineralization by C-type natriuretic peptide in osteoblastic cells. J Biochem 125:103–108
23. Suda M, Komatsu Y, Tanaka K, Yasoda A, Sakuma Y, Tamura N, Ogawa Y, Nakao K (1999) C-type natriuretic peptide/guanylate cyclase B system in rat osteogenic ROB-C26 cells and its down-regulation by dexamethazone. Calcif Tissue Int 65:472–478
24. Inoue A, Kamiya A, Ishiji A, Hiruma Y, Hirose S, Hagiwara H (2000) Vasoactive peptide-regulated gene expression during osteoblastic differentiation. J Cardiovasc Pharmacol 36:S286–S289
25. Inoue A, Kobayashi Y, Ishizuka M, Hirose S, Hagiwara H (2002) Identification of a novel osteoblastic gene, inducible by C-type natriuretic peptide, whose transcript might function in mineralization as a noncoding RNA. Calcif Tissue Int 70:111–116
26. Yeh LC, Zavala MC, Lee JC (2006) C-type natriuretic peptide enhances osteogenic protein-1-induced osteoblastic cell differentiation via Smad5 phosphorylation. J Cell Biochem 97:494–500
27. Kaneki H, Kurokawa M, Ide H (2008) The receptor attributable to C-type natriuretic peptide-induced differentiation of osteoblasts is switched from type B- to type C-natriuretic peptide receptor with aging. J Cell Biochem 103:753–764
28. Holliday LS, Dean AD, Greenwald JE, Glucks SL (1995) C-type natriuretic peptide increases bone resorption in 1,25-dihydroxyvitamin D_3–stimulated mouse bone marrow cultures. J Biol Chem 270:18983–18989
29. Hachiya R, Ohashi Y, Kamei Y, Suganami T, Mochizuki H, Mitsui N, Saitoh M, Sakuragi M, Nishimura G, Ohashi H, Hasegawa T, Ogawa Y (2007) Intact kinase homology domain of natriuretic peptide receptor-B is essential for skeletal development. J Clin Endocrinol Metab 92:4009–4014
30. Superti-Furga A, Unger S (2007) Nosology and classification of genetic skeletal disorders: 2006 revision. Am J Med Genet A 143:1–18
31. Olney RC, Bükülmez H, Bartels CF, Prickett TC, Espiner EA, Potter LR, Warman ML (2006) Heterozygous mutations in natriuretic peptide receptor-B (NPR2) are associated with short stature. J Clin Endocrinol Metab 91:1229–1232

Forkhead Box A1 (FOXA1) and A2 (FOXA2) Oppositely Regulate Human Type 1 Iodothyronine Deiodinase Gene in Liver

Naotetsu Kanamoto, Tetsuya Tagami, Yoriko Ueda-Sakane, Masakatsu Sone, Masako Miura, Akihiro Yasoda, Naohisa Tamura, Hiroshi Arai, and Kazuwa Nakao

Department of Medicine and Clinical Science, Kyoto University Graduate School of Medicine (N.K., Y.U.-S., M.S., M.M., A.Y., N.T., H.A., K.N.), Kyoto 606-8507, Japan; and Division of Endocrinology and Metabolism, Clinical Research Institute, National Hospital Organization Kyoto Medical Center (T.T.), Kyoto 612-8555, Japan

Type 1 iodothyronine deiodinase (D1), a selenoenzyme that catalyzes the bioactivation of thyroid hormone, is expressed mainly in the liver. Its expression and activity are modulated by several factors, but the precise mechanism of its transcriptional regulation remains unclear. In the present study, we have analyzed the promoter of human D1 gene (*hDIO1*) to identify factors that prevalently increase D1 activity in the human liver. Deletion and mutation analyses demonstrated that a forkhead box (FOX)A binding site and an E-box site within the region between nucleotides −187 and −132 are important for *hDIO1* promoter activity in the liver. EMSA demonstrated that FOXA1 and FOXA2 specifically bind to the FOXA binding site and that upstream stimulatory factor (USF) specifically binds to the E-box element. Overexpression of FOXA2 decreased *hDIO1* promoter activity, and short interfering RNA-mediated knockdown of FOXA2 increased the expression of *hDIO1* mRNA. In contrast, overexpression of USF1/2 increased *hDIO1* promoter activity. Short interfering RNA-mediated knockdown of FOXA1 decreased the expression of *hDIO1* mRNA, but knockdown of both FOXA1 and FOXA2 restored it. The response of the *hDIO1* promoter to USF was greatly attenuated in the absence of FOXA1. Taken together, these results indicate that a balance of FOXA1 and FOXA2 expression modulates *hDIO1* expression in the liver. **(*Endocrinology* 153: 492–500, 2012)**

Thyroid hormone activation and inactivation are mediated by three selenoenzymes, type 1 iodothyronine deiodinase (D1), D2, and D3. D1 and D2 catalyze the conversion of T_4 to T_3 via removal of outerring iodine (1). The human D1 gene (*hDIO1*) is expressed in the liver, kidney, thyroid, and pituitary (2). The D2 gene is expressed in the central nervous system, pituitary, heart, and skeletal muscle, but it is absent in the liver (1). The D3 gene is expressed in the central nervous system and placenta, and it is involved in thyroid hormone inactivation by mediating the removal of innerring iodine. Unlike D2, D1 activity is considered to be regulated predominantly at the pretranslational level. The expression and activity of D1 are modulated by a variety of factors. T_3 induces the expression of *hDIO1* via two thyroid hormone responsive elements within its promoter (3), and nuclear factor κB induced by TNFα inhibits the T_3-dependent induction of D1 (4). However, the precise mechanism of the transcriptional regulation of *hDIO1* expression remains unclear.

In this study, we sought to identify factors that increased D1 activity in the liver, a main organ that expresses *hDIO1*. We assessed the promoter activity of the 5-kb 5′-flanking region of *hDIO1* and characterized regulatory element-binding proteins within this region. In this study, we identify responsive elements for the forkhead box (FOX) transcription factors FOXA1/FOXA2 and the ba-

ISSN Print 0013-7227 ISSN Online 1945-7170
Printed in U.S.A.

doi: 10.1210/en.2011-1310 Received May 30, 2011. Accepted October 17, 2011.
First Published Online November 8, 2011

Abbreviations: D1, Type 1 iodothyronine deiodinase; FOX, forkhead box; *hDIO1*, human D1 gene; HNF, hepatocyte nuclear factor; MUT, mutated oligonucleotide; siRNA, short interfering RNA; USF, upstream stimulatory factor; WT, wild type.

sic/helix-loop-helix-leucine zipper transcription factor upstream stimulatory factor (USF), and we show that FOXA1, FOXA2, and USF all participate in the regulation of *hDIO1*. We also show that FOXA1 is required for the activation of the *hDIO1* promoter by USF and that FOXA2 represses the transcription of *hDIO1* and disrupts the interaction of USF with FOXA1 by occupying the FOXA binding site. Collectively, these results demonstrate that FOXA1 and FOXA2 display opposing activity in the regulation of *hDIO1* expression in the liver.

Materials and Methods

Cell culture

The human liver carcinoma cell line HepG2 was obtained from American Type Culture Collection (Manassas, VA) and cultured in MEM (Life Technologies, Carlsbad, CA) with 0.1 mM nonessential amino acid solution (Life Technologies), 1 mM sodium pyruvate (Life Technologies), 100 U/ml penicillin, 100 μg/ml streptomycin, and 0.25 μg/ml amphotericin B supplemented with 10% fetal bovine serum (Sigma-Aldrich, St. Louis, MO) at 37 C in a humidified atmosphere containing 5% CO_2. TSA 201 cells, a clone of human embryonic kidney 293 cells (5), were cultured in DMEM (Life Technologies) with 100 U/ml penicillin, 100 μg/ml streptomycin, and 0.25 μg/ml amphotericin B supplemented with 10% fetal bovine serum at 37 C in a humidified atmosphere containing 5% CO_2.

Plasmid construction

Deletion mutants of the 5′-flanking regions of *hDIO1* (−4949, −2023, −343, −187, −150, −131, and −103/−4, the translational start site was set at +1) were prepared by PCR using human genomic DNA from leukocytes as a template. The resulting PCR products were subcloned into *Eco*RV or *Kpn*I/*Hin*dIII-digested pGL4.10 (Promega, Madison, WI) to create a fusion with the luciferase gene (−4949, −2023, −343, −187, −150, −131, and −103/−4 hDIO1-Luc). The PCR primers, containing *Eco*RV, *Kpn*I, or *Hin*dIII linker, are listed in Table 1. The correct orientation of these deletion mutant constructs was confirmed by sequencing.

Mutations were created using the QuikChange Site-Directed Mutagenesis kit (Stratagene, La Jolla, CA), according to the manufacturer's instruction; −187/−4 and −150/−4 hDIO1-Luc were used as templates. For mutagenesis, the sequences of the FOXA binding element and E-box were specified in figure 3 below. Mutated constructs were isolated from each reaction and verified by sequencing.

Plasmids expressing cDNA for FOXA2 and USF1, pF1KB7038 and pF1KB8339, respectively, were generated by Kazusa DNA Research Institute (Chiba, Japan) and purchased from Promega. These plasmids were digested with *Sgf*I and *Pme*I, and cDNA for FOXA2 and USF1 were ligated into the *Sgf*I/*Pme*I-digested pF4A CMV Flexi vector (Promega), which uses the human cytomegalovirus intermediate-early enhancer/promoter to allow constitutive protein expression at native levels in mammalian cells. The open reading frame of human USF2 was generated by PCR using HeLa cell cDNA as a template. The PCR primers containing *Sgf*I or *Pme*I linker are listed in Table 1. The PCR product was digested with *Sgf*I and *Pme*I, cloned into the *Sgf*I/*Pme*I-digested pF4A CMV Flexi vector, and verified by sequencing.

Transient transfection and luciferase assay

HepG2 and TSA 201 cells were plated at 1.5–2 × 10^5 and 0.5–1 × 10^5 cells/well in 24-well tissue culture plates, respectively. Cells were maintained in 0.5 ml of antibiotic-free medium for 1 d before transfection. Transient transfections were performed using the Lipofectamine LTX reagent (Life Technologies) for HepG2 cells and the Lipofectamine 2000 reagent (Life Technologies) for TSA 201 cells according to the manufacturer's instruction. In HepG2 cells, transfections included 500 ng of experimental reporter constructs and 25 ng of pGL4.74, which contained the cDNA encoding *Renilla* luciferase (Promega) as an internal control for transfection efficiency. In TSA 201 cells, transfections included 100 ng of experimental reporter constructs and 5 ng of pGL4.74. In the experiments with plasmids expressing FOXA2 and/or USF, total amount of plasmid DNA was kept constant by adding the corresponding amount of pF4A without a cDNA insert. After transfection, cells were grown in antibiotic-free medium and harvested after 48 h. Luciferase activity was determined using the Dual-Luciferase Reporter Assay System (Promega), and luminescence was measured by a 2030 ARVOX multilabel reader (PerkinElmer, Waltham, MA). Firefly luciferase activity was normalized to *Renilla* luciferase activity in each well to control for transfection efficiency.

Computational analysis of the putative transcription factor binding sites

The putative transcription factor binding sites on the 5′-flanking region of *hDIO1* were identified by computational

TABLE 1. Oligonucleotides used in plasmid construction and RT-PCR

	Forward primer (5′-3′)	Reverse primer (5′-3′)	Accession no.
Plusmid construction			
−4949/−4 hdio1-Luc	GGGGATATCGCAGGTGCAGCCTAGAGATGTAACG	CCCAAGCTTGGCAAAGCCAGAGTAAGCTC	AL031427
−2023/−4 hdio1-Luc	CGGGGTACCACACTTCCATTCCAGTTACAG	CCCAAGCTTGGCAAAGCCAGAGTAAGCTC	AL031427
−343/−4 hdio1-Luc	CGGGGTACCGAGAGAGCATCTAACAGGTTC	CCCAAGCTTGGCAAAGCCAGAGTAAGCTC	AL031427
−187/−4 hdio1-Luc	CGGGGTACCGACCTTTGTGCACCTGGTTAG	CCCAAGCTTGGCAAAGCCAGAGTAAGCTC	AL031427
−150/−4 hdio1-Luc	CGGGGTACCGACAGAAAGGCAAACATCTTC	CCCAAGCTTGGCAAAGCCAGAGTAAGCTC	AL031427
−131/−4 hdio1-Luc	CGGGGTACCTCTGACCTGACTCCTTCCCCTG	CCCAAGCTTGGCAAAGCCAGAGTAAGCTC	AL031427
−103/−4 hdio1-Luc	CGGGGTACCGGTTGGCTGCTCCTACCCTGC	CCCAAGCTTGGCAAAGCCAGAGTAAGCTC	AL031427
pF4A-USF2	AGCAGCGATCGCCATGGACATGCTGGACCCGGGTCTGGA	CGAGGTTTAAACCTGCCGGGTGCCCTCGCCCA	NM_003367
RT-PCR			
hDIO1	CAGAGTCAAGCGGAACATCC	CCGTTGGTCACCTAGAATTG	NM_000792
Cyclophilin A	GCACTGGAGAGAAAGGATTTGG	CAGCAATGGTGATCTTCTTGC	NM_021130

analysis using TFSEARCH databases (http://www.cbrc.jp/research/db/TFSEARCHJ.html), based on the TRANSFAC databases (6).

RNA isolation, RT-PCR, and quantitative PCR

Total RNA was extracted from HepG2 cells using the RNeasy Plus Mini kit (QIAGEN, Valencia, CA) according to the manufacturer's instruction. One microgram of total RNA was reverse transcribed with random hexamers using a First-strand cDNA Synthesis kit (GE Healthcare UK Ltd., Buckinghamshire, UK) according to the manufacturer's instruction. The resulting cDNA were diluted 1:10 and subjected to PCR amplification with 0.5 mM each of the sense and antisense primers and 0.5 U of AmpliTaq Gold DNA polymerase (Life Technologies). The PCR primers used for *hDIO1* and human cyclophilin A gene are indicated in Table 1. The PCR conditions were 40 cycles of denaturation for 1 min at 95 C, annealing for 1 min at 52 C, and extension for 1 min at 72 C. The PCR products were electrophoresed in 2% agarose gels.

Quantitative PCR reactions were performed, recorded, and analyzed using TaqMan Gene Expression Assays with StepOnePlus real-time PCR system (Life Technologies). The probe and primers were Hs00270129_m1 (human *FOXA1*), Hs00232764_m1 (human *FOXA2*), and Hs00174944_m1 (*hDIO1*) and purchased from Life Technologies. Diluted cDNA were amplified using the following conditions: 50 C for 2 min, 95 C for 10 min, and 40 cycles of 95 C for 15 sec and 60 C for 1 min, followed by continuous incubation at 25 C. Expression levels of FOXA1, FOXA2, and hDIO1 were normalized to cyclophilin A to compensate for variations in input RNA.

Preparation of cell extracts and EMSA

Nuclear extracts were prepared from HepG2 cells using the Nuclear Extract kit (Active Motif, Carlsbad, CA), according to the manufacturer's instruction. EMSA were conducted using a LightShift chemiluminescent EMSA kit (Thermo Fisher Scientific, Rockford, IL) with slight modifications of the original manufacturer's instruction. Oligonucleotides 3′-end labeled with biotin were synthesized (Life Technologies) and annealed to generate double-stranded oligonucleotide probes. Two hundred femtomoles of oligonucleotide probe were incubated with 10–15 μg of nuclear protein and 0.5 μg of poly (dI-dC) in the presence or absence of competing oligonucleotide in 10× binding buffer [containing 100 mM Tris, 500 mM KCl, and 10 mM dithiothreitol (pH 7.5)] and 75 mM KCl, and 5% glycerol was added to solutions containing probes with an E-box element. After a 30-min incubation at room temperature, DNA-protein complexes were separated by electrophoresis on a 6% DNA retardation gel (Life Technologies) at 4 C in 0.5× Tris-borate, EDTA buffer [containing 89 mM Tris-borate and 2 mM EDTA (pH 8.0)]. For supershift assays, binding reactions were incubated for 45 min at room temperature with antibodies before the addition of labeled probes. The antibodies used in the supershift assays were as follows: 1 μl (200 μg/0.1 ml) of USF1 (sc-8983X), USF2 (sc-861X), E47 (sc-763X), FOXA1 (sc-6553X), FOXA2 (sc-6554X), and FOXA3 (sc-5361X) and 5 μl (200 μg/0.5 ml) of normal goat and normal rabbit IgG, and all were purchased from Santa Cruz Biotechnology, Inc. (Santa Cruz, CA). After electrophoresis, samples were transferred onto nylon membranes and fixed by UV irradiation. Biotinylated DNA was detected using a Fujix Lumino-image analyzer (LAS-1000; Fuji Photo Film Co., Ltd., Tokyo, Japan).

Transfection of short interfering RNA (siRNA)

An aliquot of 6 pmol siRNA specific for FOXA1 and/or FOXA2 (Stealth Select RNAi, Life Technologies) or a negative control siRNA (Stealth RNAi Negative Control, Life Technologies) was transfected into HepG2 cells using the Lipofectamine RNAiMax reagent (Life Technologies) by reverse transfection according to the manufacturer's instruction. After transfection, HepG2 cells were plated at 1.5–2 × 10^5 cells/well in 24-well tissue culture plates and maintained in 0.5 ml of antibiotic-free medium for 24–48 h. mRNA extraction and analysis were performed as described above.

Statistics

The data represent the mean ± SEM and were obtained from at least three separate experiments, each performed in triplicate. Statistical analyses were performed to examine the significance of differences among the results using unpaired *t* test or ANOVA followed by Student-Newman-Keuls test or Dunnett's test.

Results

Functional analysis of the 5′-flanking region of the *hDIO1* gene

To identify regions within the promoter region of *hDIO1* important for regulating its expression, a series of 5′-deletion constructs was subcloned into the pGL4.10 vector and transiently transfected into HepG2 and TSA 201 cells (Fig. 1A). In both HepG2 and TSA 201 cells, luciferase activity increased by deletion of nucleotides −150 to −131 and decreased after deletion of −131 to −103. Among the tested constructs, the luciferase activity produced by transfection of −150/−4 hDIO1-Luc was specifically and markedly decreased in HepG2 cells. Additionally, more pronounced differences were seen between the activity of −150/−4 hDIO1-Luc and −131/−4 hDIO1-Luc in HepG2 cells compared with TSA 201 cells. In addition, luciferase activity was markedly increased by deleting the region from −343 to −187 and decreased after deletion of −187 to −150 only in HepG2 cells. Taken together, these results indicate that the region between nucleotides −187 and −132 is important for *hDIO1* promoter function in HepG2 cells. To confirm the expression of *hDIO1*, we performed RT-PCR using total RNA isolated from HepG2 and TSA 201 cells, a liver and kidney cell line, respectively. As shown in Fig. 1B, although there was a difference in the degree of gene expression, *hDIO1* was expressed in both cell lines; this was consistent with a previous report examining *hDIO1* tissue distribution (2). Additionally, multiple PCR products were detected, because there are several alternative splice variants of *hDIO1* (7). These results indicate that there may exist a sequence

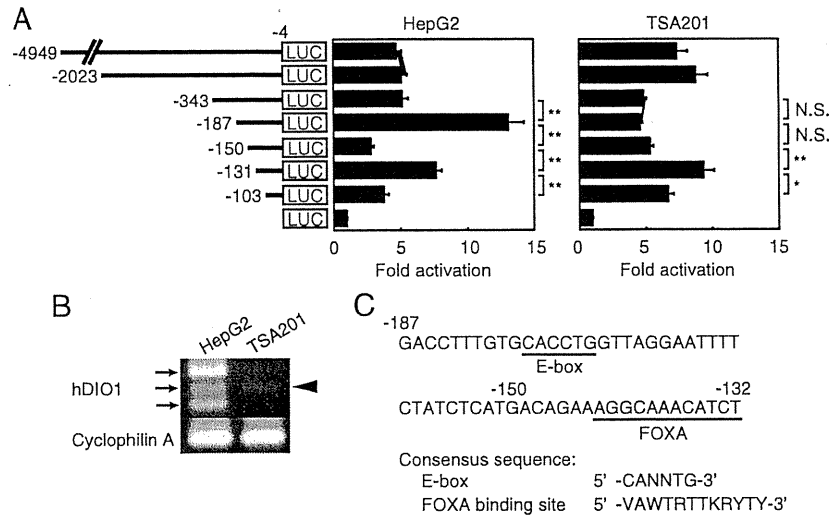

FIG. 1. Liver-specific changes in *hDIO1* promoter activity. A, A series of 5′-deletion constructs of the *hDIO1* promoter were transiently transfected into HepG2 or TSA 201 cells. Promoter activity was normalized to *Renilla* luciferase activity and expressed as the relative activity to promoterless pGL4.10. Statistical significance was determined by ANOVA followed by Student-Newman-Keuls test. *, $P < 0.05$; **, $P < 0.01$. N.S., Not significant. B, RT-PCR analysis of *hDIO1* expression. Electrophoretic analysis of RT-PCR products using total RNA from HepG2 and TSA 201 cells was performed. The *arrows* and *arrowhead* correspond to the RT-PCR products using total RNA from HepG2 and TSA 201 cells, respectively. Cyclophilin A was used as a positive control. C, The nucleotide sequences of the 5′-flanking region of *hDIO1* are shown. The translational start site was set at +1. *Underlined sequences* indicate putative binding sites for transcription factors. Consensus sequences of E-box site and FOXA binding site are shown at the *bottom*. Abbreviations for nucleotides: W (A or T), K (G or T), Y (C or T), R (A or G), V (A, C, or G), and N (A, C, G, or T). LUC, Luciferase.

essential for liver-specific expression of *hDIO1* within the −187 to −132 region of its promoter. A computational analysis of this region revealed the presence of a consensus E-box site between nucleotides −187 and −151 and a FOXA binding site between nucleotides −150 and −132 (Fig. 1C).

Promoter activity associated with the FOXA binding site and the E-box

To better understand the contribution of the FOXA binding site and the E-box on the expression of *hDIO1* in liver-derived HepG2 cells, we examined luciferase activity in cells transfected with wild-type (WT) or mutated *hDIO1* promoter constructs. In HepG2 cells, luciferase activity was increased 2-fold by mutating the FOXA binding site when cells were transfected with a −150/−4 hDIO1-Luc construct (Fig. 2A). In addition, when cells were transfected with a −187/−4 hDIO1-Luc construct, luciferase activity was nearly completely lost by destruction of the E-box, and mutation of the FOXA binding site caused a decrease in luciferase activity by 50% (Fig. 2B). In TSA 201 cells transfected with −187/−4 hDIO1-Luc, luciferase activity was almost completely abolished by mutation of the E-box, but mutation of the FOXA binding site in both −187/−4 hDIO1-Luc and −150/−4 hDIO1-Luc did not significantly affect luciferase activity (Fig. 2). Thus, the E-box present within the *hDIO1* promoter is required for the enhancer activity in both liver- and kidney-derived cells, but the FOXA binding site exhibits liver-specific enhancer and repressor activity.

Binding of FOXA1/FOXA2 to the FOXA binding site and USF to the E-box

To determine the transcription factors that bind to these elements in the promoter of *hDIO1* in HepG2 cells, we performed EMSA using oligonucleotides with the FOXA binding site and the E-box. Incubation of HepG2 cell extracts with oligonucleotides containing the FOXA binding site (Fig. 3A, WT-F) led to the formation of several DNA/protein complexes (Fig. 3B, lane 2). Formation of one of these complexes was inhibited by incubation with excess WT-F, but not mutated oligonucleotide (MUT)-F, demonstrating the specificity of this complex (Fig. 3B, lanes 3–6). Additionally, the complex was supershifted by addition of anti-FOXA1 and anti-FOXA2 antibodies (Fig. 3B, lanes 7 and 8). However, an antibody specific for FOXA3, which binds an identical sequence, or normal goat IgG did not disrupt complex formation (Fig. 3B, lanes 9 and 10). These results suggest that the putative FOXA binding site is specifically bound by FOXA1 or FOXA2. We next examined binding to the E-box sequence, and several complexes were formed by

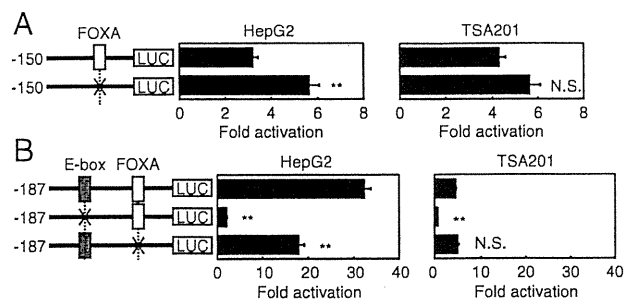

FIG. 2. Changes in *hDIO1* promoter activity by FOXA binding site and E-box. Schematic diagram in the *left* of each figure representing WT and site-specific mutations of the *hDIO1* promoter, introduced into the upstream region of the luciferase gene. A *cross* represents the site-specific mutation of the putative FOXA binding site or E-box. Each construct was transiently transfected into HepG2 or TSA 201 cells. Promoter activity was normalized to *Renilla* luciferase activity and expressed as the relative activity to promoterless pGL4.10. Statistical significance was determined by unpaired *t* test (A) or ANOVA followed by Dunnett's test (B). **, $P < 0.01$. N.S., Not significant.

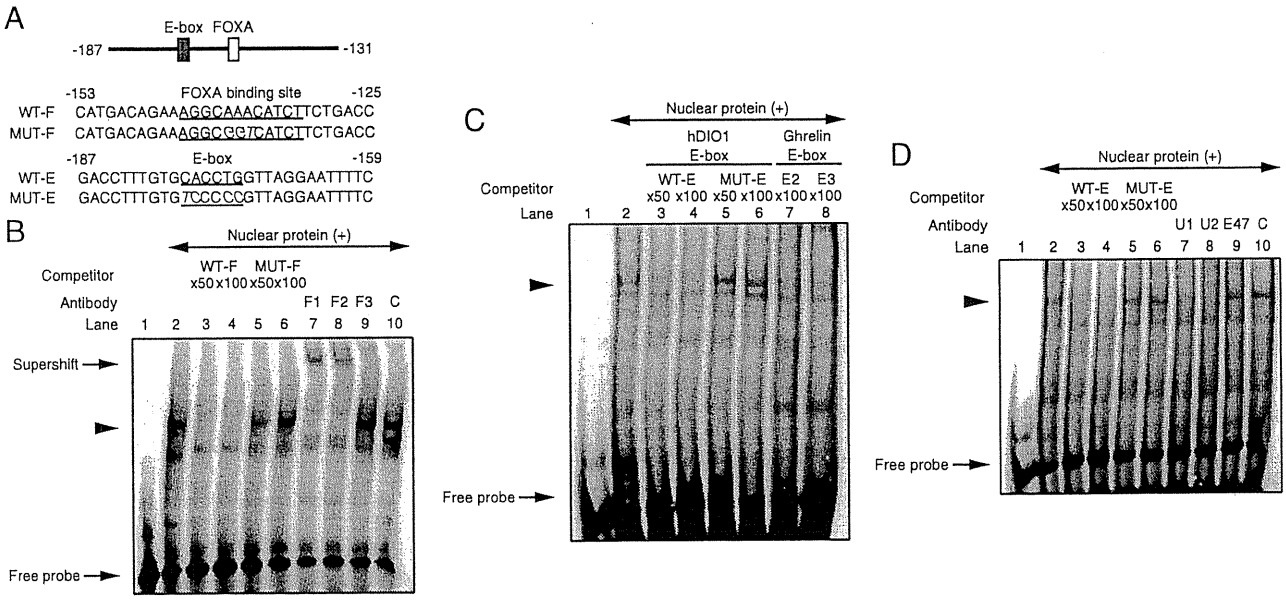

FIG. 3. Specific binding of the transcription factors within the −187 and −132 region in the *hDIO1* promoter using nuclear proteins from HepG2 cells. Panel A, Sequences of the double-stranded oligonucleotides used in EMSA. WT-F, WT *hDIO1* sequence identical to the −153 to −125 region, containing the FOXA binding site at −143 to −132. MUT-F contains a mutated FOXA binding site. WT-E, WT *hDIO1* sequence identical to the −187 to −159 region, containing the E-box at −177 to −172. MUT-E contains a mutated E-box. Each putative binding site is *underlined*; the mutated base pairs are indicated by *italic letters*. Panel B, Oligonucleotide WT-F was used as the probe for EMSA either without competitor (lane 2) or in the presence of 50- and 100-fold molar excesses of unlabeled WT-F (lanes 3 and 4, respectively) or MUT-F (lanes 5 and 6, respectively). The specific complex formed from HepG2 cell nuclear extract and WT-F is indicated by an *arrowhead*. Supershift assay experiments were performed using antibody against FOXA1 (F1; lane 7), FOXA2 (F2; lane 8), or FOXA3 (F3; lane 9) and normal goat IgG (C; lane 10). Panel C, Oligonucleotide WT-E was used as the probe for EMSA either without competitor (lane 2) or in the presence of 50- and 100-fold molar excesses of unlabeled WT-E (lanes 3 and 4, respectively), MUT-E (lanes 5 and 6, respectively), or 100-fold molar excesses of unlabeled E-box from the human ghrelin gene [E2 and E3 (in Ref. 8); lanes 7 and 8, respectively]. The specific complex formed from HepG2 cell nuclear extract and WT-E is indicated by an *arrowhead*. D, Supershift assay experiments were performed using antibody against USF1 (U1; lane 7), USF2 (U2; lane 8), or E47 (E47; lane 9) and normal rabbit IgG (C; lane 10). C, Negative control (normal goat and normal rabbit IgG).

incubation of HepG2 cell extracts with an appropriate oligonucleotide (Fig. 3A, WT-E, and C, lane 2). Formation of one of these complexes was inhibited by incubating with an excess of WT-E and the E-box from human ghrelin gene (8) but not by a mutant oligonucleotide MUT-E (Fig. 3C, lanes 3–8). Computational analysis predicted that the putative E-box site binds the basic/helix-loop-helix-leucine zipper transcription factor USF, and to investigate this hypothesis, a supershift assay was performed using antibodies specific for USF1 and USF2. Addition of antibodies specific for USF1 and USF2 completely inhibited complex formation (Fig. 3D, lanes 7 and 8). However, incubation with an antibody against E47, a protein that binds a similar E-box sequence, or normal rabbit IgG did not disrupt complex formation (Fig. 3D, lanes 9 and 10). These results suggest that USF1/USF2 bind the putative E-box, and this complex likely contains a USF1/USF2 heterodimer. Collectively, FOXA1, FOXA2, and USF likely participate in the regulation of *hDIO1* expression.

Effect of overexpression of FOXA2 or USF on *hDIO1* promoter activity

To determine whether FOXA and USF have the potential to affect the activity of the *hDIO1* promoter in liver cells, a −187/−4 hDIO1-Luc construct was transiently transfected into HepG2 cells along with increasing amounts of either a FOXA2 or USF expression plasmid. The luciferase activity decreased in a dose-dependent manner by cotransfection of the FOXA2 expression plasmid with −187/−4 hDIO1-Luc (Fig. 4A). In contrast, luciferase activity increased dose dependently by the cotransfection of the USF1 or USF2 expression plasmid, and overexpression of USF2 consistently led to greater *hDIO1* promoter activity than expression of USF1 alone (Fig. 4B). Thus, transcription of *hDIO1* is negatively regulated by FOXA2 and positively regulated by USF. Although we transiently transfected a −187/−4 hDIO1-Luc construct into HepG2 cells along with increasing amounts of a FOXA1 expression plasmid, we could not obtain appropriate data, indicating that the FOXA1 expression plasmid we used did not function in our experimental system for unknown reason.

RNA interference

Next, we determined the effects of FOXA on the native *hDIO1* promoter using siRNA-mediated knockdown of FOXA in HepG2 cells. As shown in Fig. 5, A and B, knock-